**Supporting Information**

# Synthesis of urea derivatives in two sequential continuous-flow reactors

*Péter Bana,[a] Ágnes Lakó,[a] Nóra Zsuzsa Kiss,[a] Zoltán Béni,[b] Áron Szigetvári,[b] János Kóti,[b] György István Túrós,[b] János Éles,[b] and István Greiner[b*]*

[a] Department of Organic Chemistry and Technology,
Budapest University of Technology and Economics, 1521 Budapest, Hungary
[b] Gedeon Richter Plc., 1475 Budapest, PO Box 27, Hungary

## Table of contents

Pictorial description of the flow system ..... S2

Set-up for the attempted standalone optimization of the isocyanate formation ..... S3

FT-IR spectra of reaction mixtures ..... S3

Optimization of the flow synthesis of urea **7a** ..... S4

Procedure for urea synthesis using basic ion-exchange resin in the second reaction step ..... S5

Procedure for measuring the free internal volume of the packed bed reactor ..... S6

Investigation of the mechanistic role of the applied base ..... S6

NMR analysis of the crude batch reaction mixture ..... S7

Procedure for screening of the applicable bases in the first reaction step of the urea synthesis ..... S8

Procedure for urea synthesis using *N*,*N*-diisopropylethylamine (DIPEA) in the first reaction step ..... S9

Detailed parameters of the flow syntheses of ureas (**7a-j**, **3)** ..... S10

Characterization data of known compounds ..... S11

NMR spectra of the isolated compounds (**7a-j**, **3)** ..... S14

References ..... S25

[*] Corresponding author. Tel: +36 1 431 4102.

*E-mail address:* i.greiner@richter.hu (I. Greiner).

## Pictorial description of the flow system

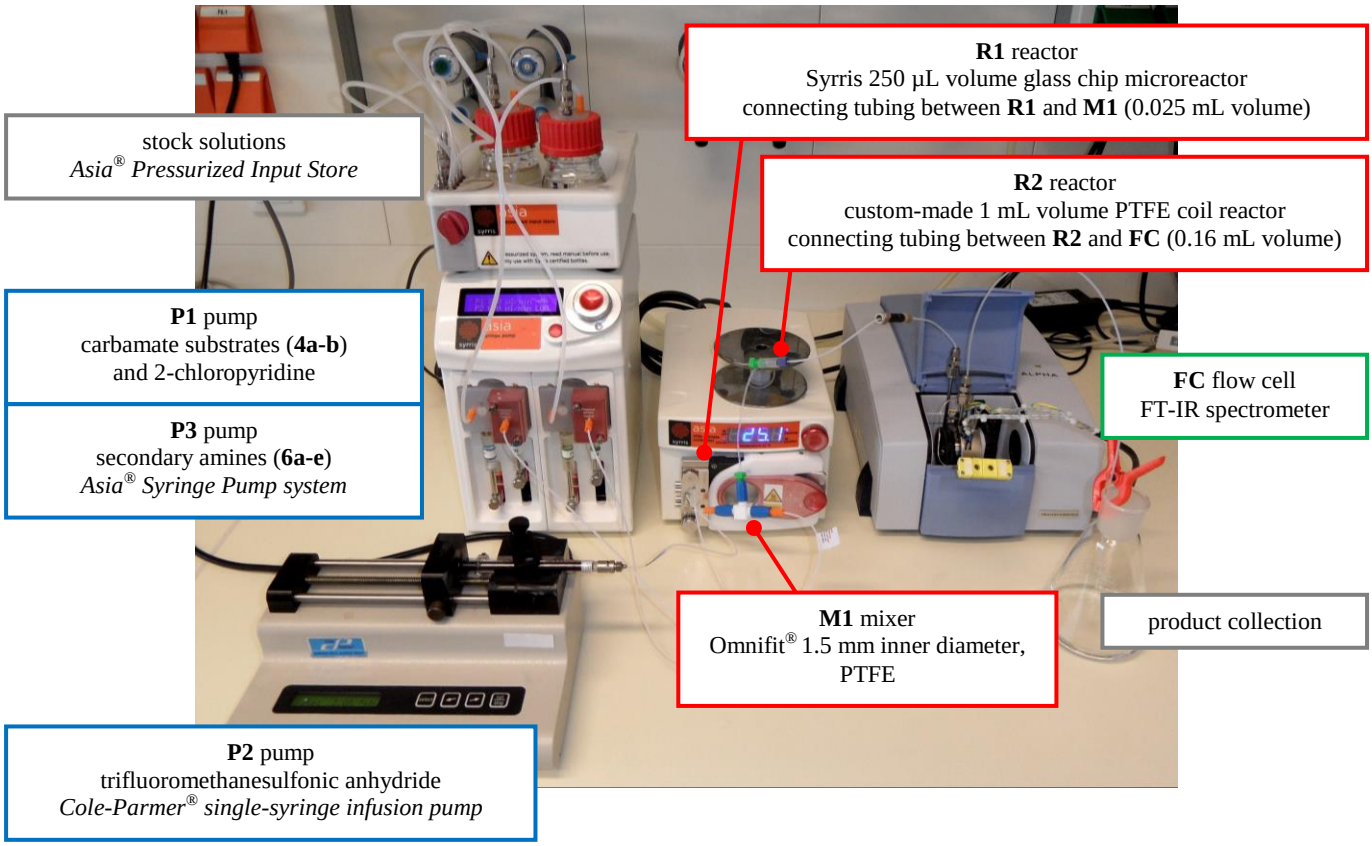


**Fig. S1.** Photograph of the flow system used throughout this study, the main components are labeled. (for details see Experimental Section)

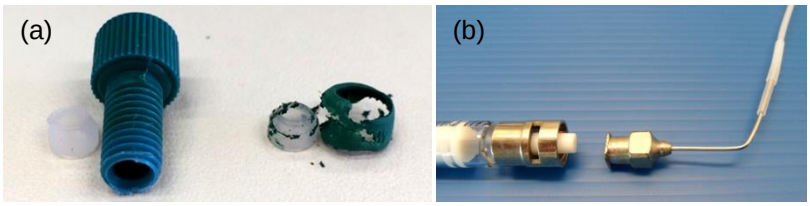


**Fig. S2.** (a) An example (before – after) of the corrosive effect of dilute solutions of $Tf_2O$ on standard plastic parts. (b) Custom made stainless steel Luer lock to tubing connector for the introduction of $Tf_2O$.

## Set-up for the attempted standalone optimization of the isocyanate formation

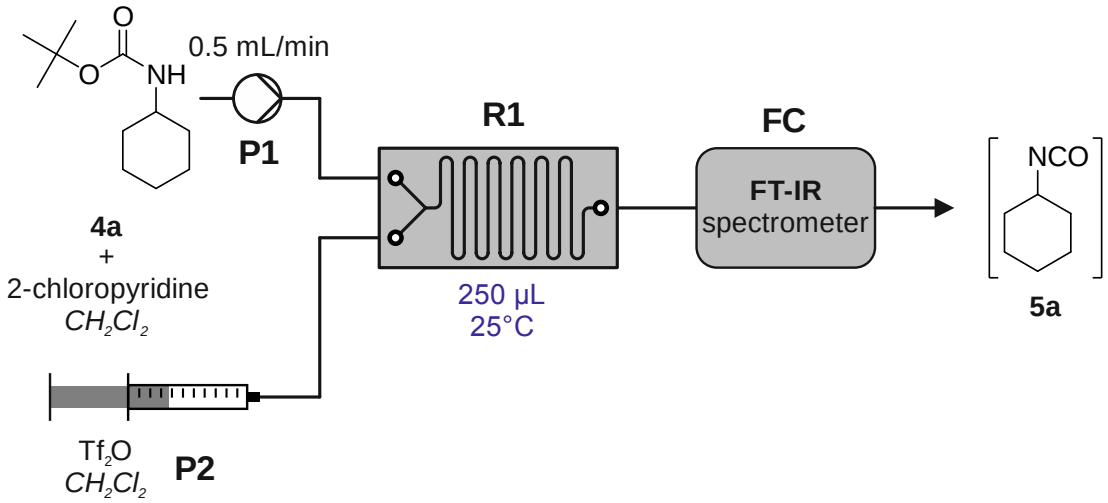


**Fig. S3.** Flow system for the in-line analysis of the reaction mixture after the isocyanate formation step

## FT-IR spectra of the reaction mixtures

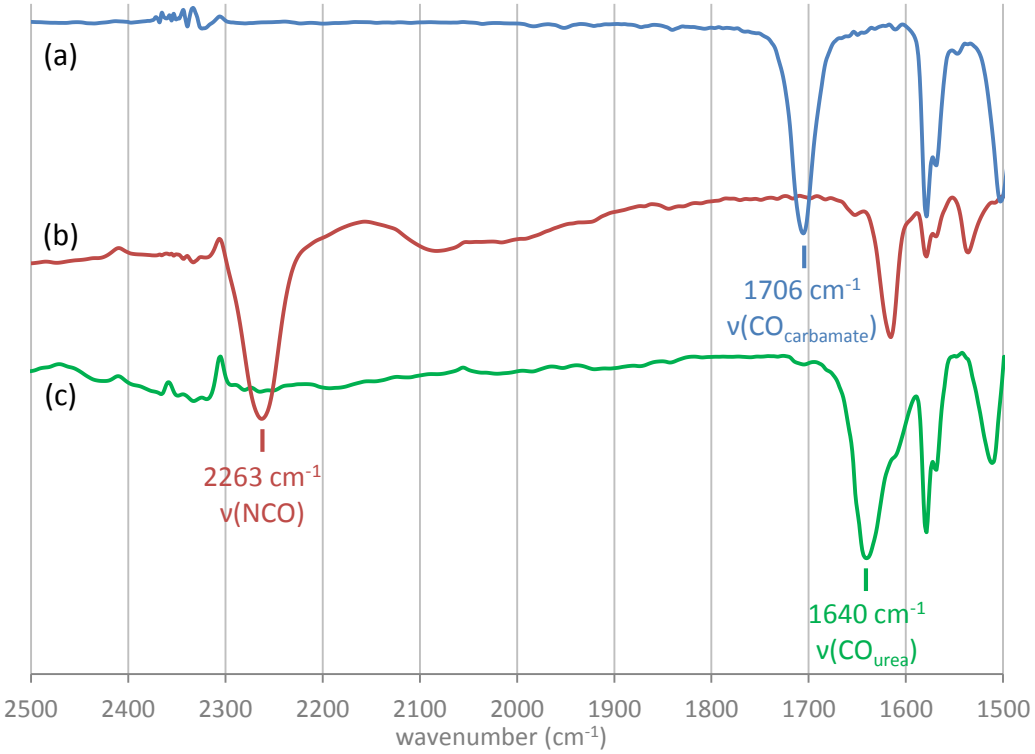


**Fig. S4.** Transmission FT-IR spectra (2500 – 1500 $cm^{-1}$ region) of the crude reaction mixtures using **4a** and **6a** as starting materials. The characteristic bands, which were used for conversion determination are marked.
(a) mixture of the starting materials before addition of $Tf_2O$ the reagent;
(b) reaction mixture after completion of the first step;
(c) reaction mixture after completion of the second step.

## Optimization of the flow synthesis of urea 7a

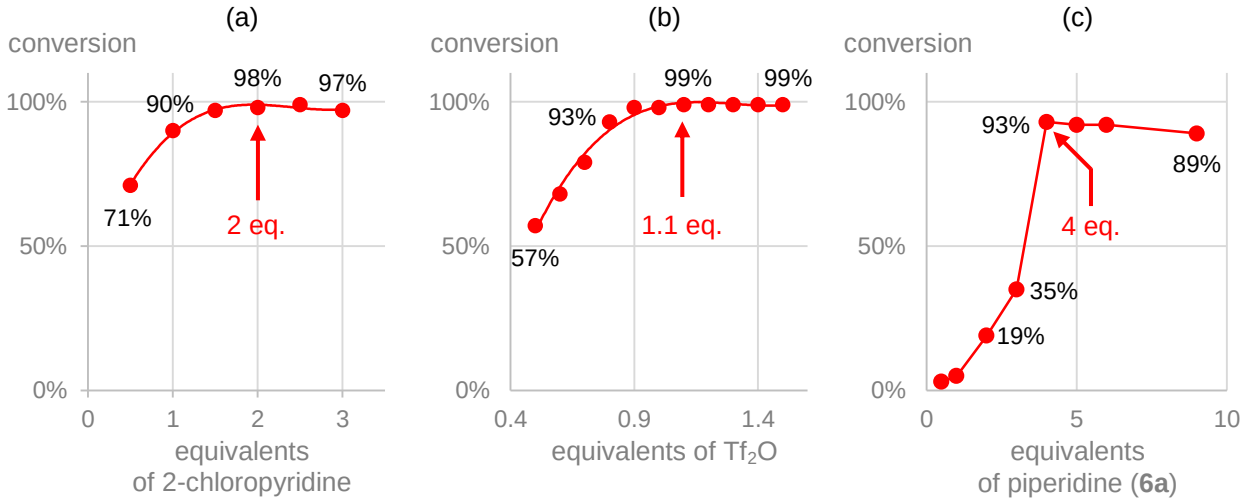


**Fig. S5.** Optimization of the reagent amounts in the model reaction.

(a) Effect of the amount of 2-chloropyridine on conversion of the first step using 1.0 eq. of $Tf_2O$.

(b) Effect of the amount of $Tf_2O$ on conversion of the first step using 2 eq. of 2-chloropyridine.

(c) Effect of the amount of piperidine (**6a**) on conversion of the second step using optimal parameters in the first step (1.1 eq. of $Tf_2O$ and 2 eq. of 2-chloropyridine).

## Procedure for urea synthesis using basic ion-exchange resin in the second reaction step

The described flow system (Fig. 2) was modified by replacing **R2** coil reactor with an Omnifit® column (**R2'**) containing ca. 1 g of Amberlyst™ A21 basic ion-exchange resin (1.6 mL free internal volume). Other parts of the system and the optimal parameters of the first step were kept unchanged (Fig. S6). Microreactors **R1**, **R2'** and mixing unit **M1** were kept at room temperature. Equivalent amount of **6a** was optimized by varying the flow rate of pump **P3**.

During optimization, the product stream was analyzed by FT-IR after reaching steady state (collecting at least 4 mL reaction mixture to the waste). Using optimal conditions, product stream was collected for 20 min (molar amount of substrate is equal to the batch procedure) in steady state operation. The crude mixture was concentrated under reduced pressure and subjected to flash chromatography. *N*-cyclohexylpiperidine-1-carboxamide (**7a**) was obtained as white crystalline solid, 53 mg, 84% yield (for characterization data see below).

Packed beds with smaller amount of ion-exchange resin did not show any benefits compared to the coil reactor.

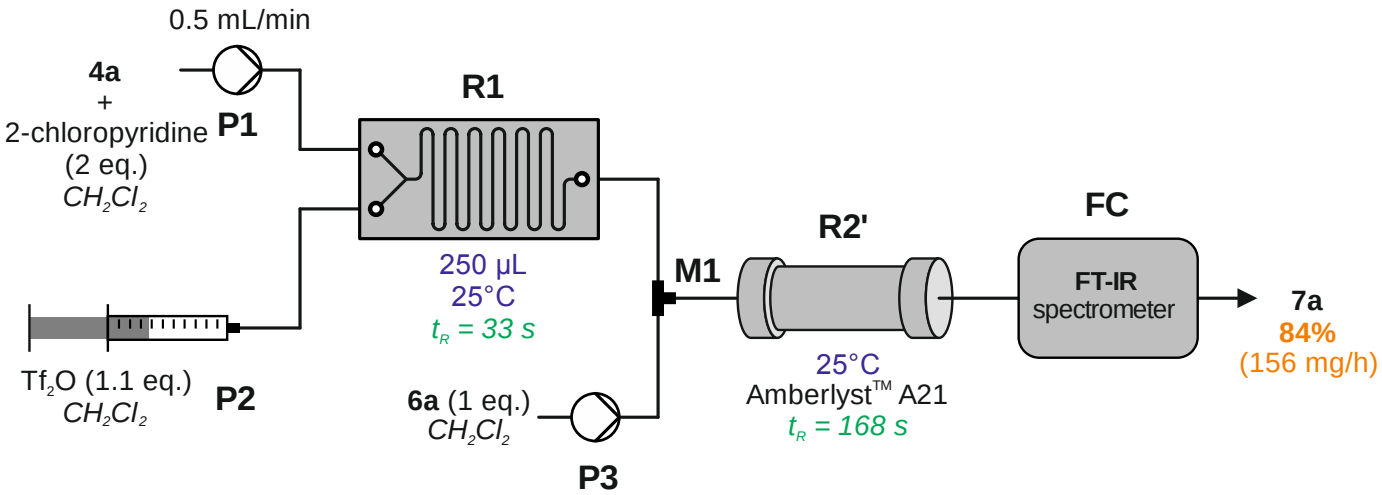


**Fig. S6.** Flow system using basic ion-exchange resin in the second step, showing optimal settings.

## Procedure for measuring the free internal volume of the packed bed reactor

The Omnifit® column (10 cm length, 6.6 mm i.d., 3.4 mL total volume) containing ca. 1 g of Amberlyst™ A21 ion-exchange resin was connected to a pump, which provided a steady flow of pure dichloromethane solvent. A small aliquot of chloroform was injected to the stream using a syringe connected through a T-piece before the column. The stream exiting the packed bed reactor was continuously analyzed using an in-line FT-IR spectrometer connected with known internal volume tubing (Fig. S7). Residence time in the packed bed reactor was calculated by subtracting the residence time in the tubing from the time elapsed between the injection and the maximal intensity of chloroform's FT-IR signal at 1520 $cm^{-1}$. Free internal volume was determined from measuring residence time using various flow rates.

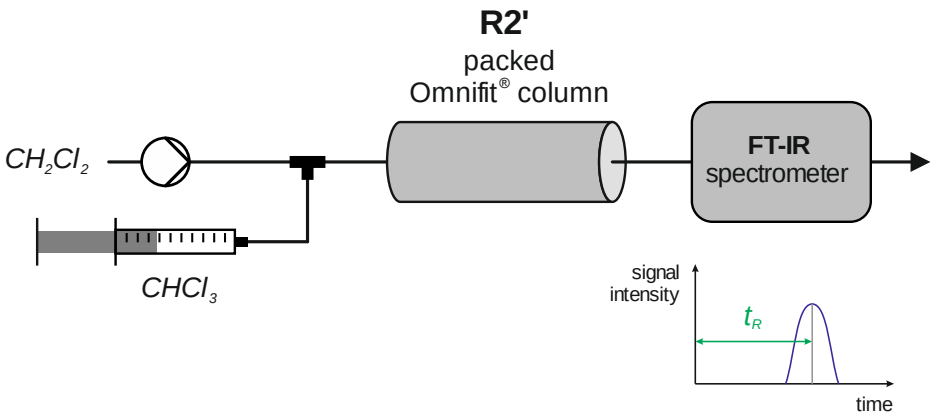


**Fig. S7.** Set-up for measuring the free internal volume of the packed bed reactor

## Investigation of the mechanistic role of the applied base

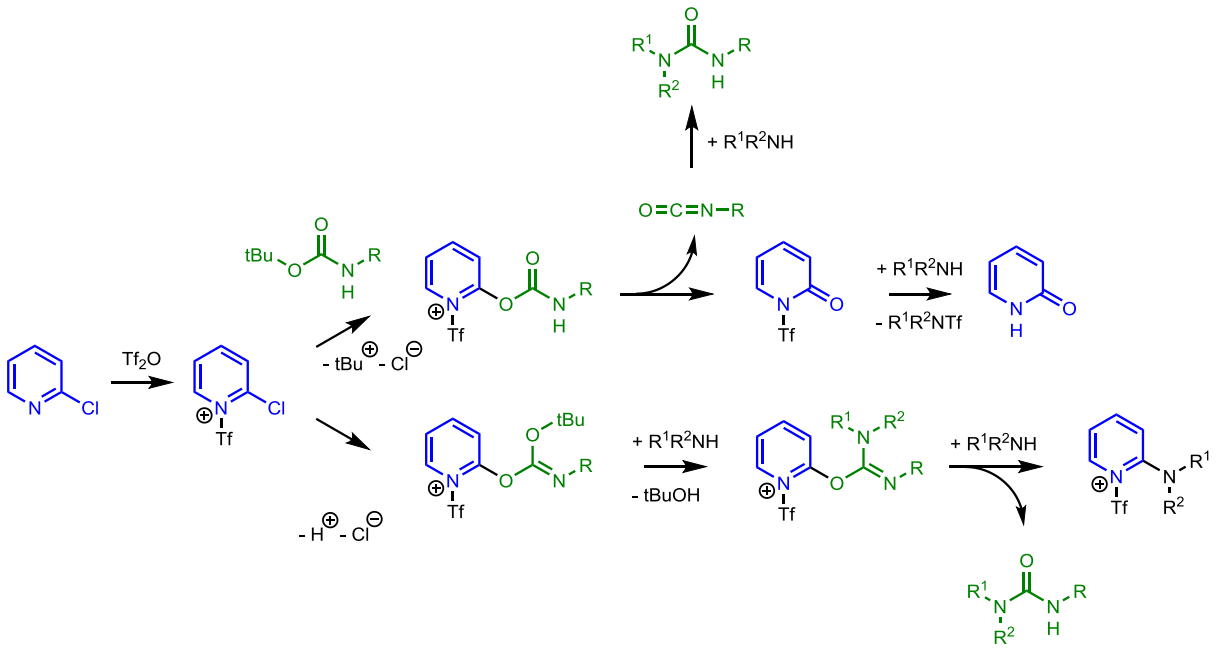


**Scheme S1.** Tentative mechanistic pathways involving a theoretical C–Cl cleavage

## NMR analysis of the crude reaction mixture of the batch process

In a 10 mL vessel, 12 mg (0.06 mmol) of *tert*-butyl cyclohexylcarbamate (**4a**) and either 18 µL (0.18 mmol; 3 eq.) or 6 µL (0.06 mmol; 1 eq.) of 2-chloropyridine was dissolved in 2.0 mL of chloroform-*d* (99.5 deut. %) under nitrogen atmosphere. 7.4 µL of *p*-xylene (0.06 mmol) was added as internal standard. 90 µL of 1M solution of trifluoromethanesulfonic anhydride in dichloromethane was added to the stirred solution.

After stirring for 50 min at room temperature. 54 µL (0.54 mmol; 9 eq.) of piperidine (**6a**) was added, the vessel was sealed using a silicone stopper and stirring was continued for 20 h at room temperature, after which 0.8 mL aliquot of the reaction mixture was filtered through a cotton plug directly into an NMR tube and analyzed by NMR immediately.

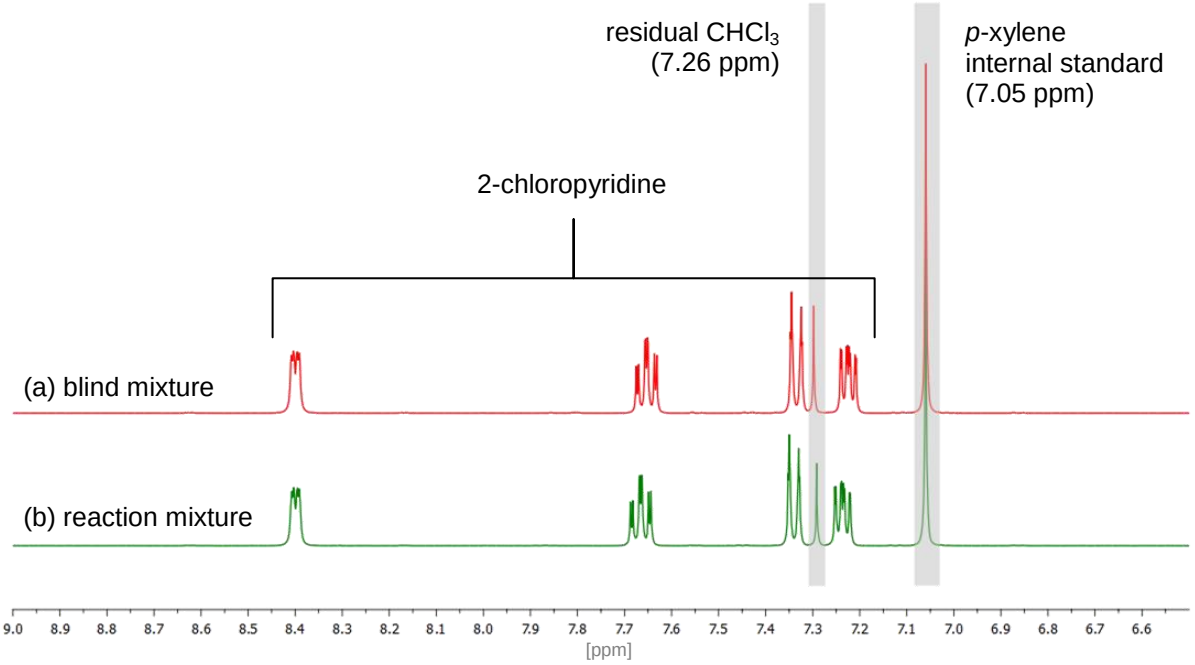


**Fig. S8.** Aromatic region (9.0 to 6.5 ppm) of the $^1$H-NMR spectra of (a) the blind mixture (b) the crude reaction mixture. 8 scan spectra are depicted for better sensitivity to show eventual impurities.

The same sequence was repeated without the addition of the trifluoromethanesulfonic anhydride reagent (blind mixtures; Fig. S8 (a); Table S1 experiment B and D), and subjected to identical conditions and analysis. Aromatic region of the $^1$H-NMR spectra of the crude reaction mixtures do not contain any signal other than 2-chloropyridine, the internal standard or the solvent (Fig. S8 (b)). Recoverable amounts of 2-chloropyridine were calculated using the amount in the crude mixture (compared to the internal standard) and the initial amount (based on accurately weighted reagents, Table S1).

**Table S1.** Recoverable amounts of 2-chloropyridine determined from the crude mixtures (based on the integral ratios of single scan $^1$H-NMR spectra).

| *experiment* | *molar amount of 2-chloropyridine* | *molar amount of $Tf_2O$* | *recoverable amount of 2-chloropyridine* | *product conversion* |
|---|---|---|---|---|
| ***A*** | 3 eq. | 1.5 eq. | **94%** | 96% |
| ***B** (blind)* | 3 eq. | – | **99%** | – |
| ***C*** | 1 eq. | 1.5 eq. | **100%** | 9% |
| ***D** (blind)* | 1 eq. | – | **99%** | – |

## Procedure for screening of the applicable bases in the first reaction step of the urea synthesis

The described flow system (Fig. 2) was extended with a Nexus 6000 infusion syringe pump (**P4**; Chemyx Inc., Stafford, TX, USA) for introduction of the neat base or (or in case of solid materials) its concentrated solution in dichloromethane, which was filled into a plastic syringe. The stream of **P1** and **P4** was combined in a T-mixer (**M2**) before entering **R1**. Other parts of the system were unchanged (Fig. S9). Microreactors **R1**, **R2** and mixing units **M1**, **M2** were kept at room temperature. Reagents were used in high excess (3 eq. of base, 1.5 eq. of $Tf_2O$ and 9 eq. of **6a**).

The product stream was analyzed by FT-IR after reaching steady state (collecting at least 4 mL reaction mixture to the waste). Conversion is based on the ratio of integrated absorbance of $\nu(CO_{carbamate})$ = 1706 cm$^{-1}$ and $\nu(CO_{urea})$ = 1640 cm$^{-1}$ bands.

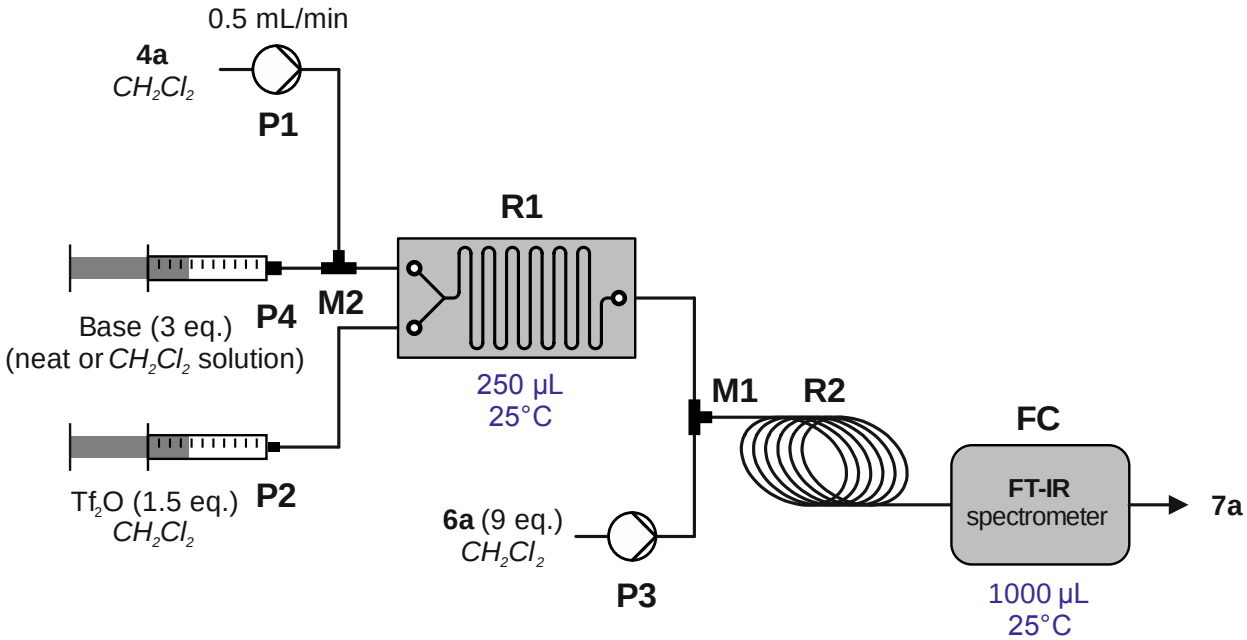


**Fig. S9.** Flow system for the screening of the applicable bases

## Procedure for urea synthesis using *N*,*N*-diisopropylethylamine (DIPEA) in the first reaction step

The described flow system (Fig. 2) was modified by replacing **R1** with a 1000 µL internal volume chip reactor (**R1'**) and extended with a Nexus 6000 infusion syringe pump (**P4**; Chemyx Inc., Stafford, TX, USA) for introduction of the neat DIPEA. The stream of **P1** and **P4** was combined in a T-mixer (**M2**) before entering **R1**. Other parts of the system were unchanged (Fig. S10). Microreactors **R1'**, **R2** and mixing units **M1**, **M2** were kept at room temperature. Flow rates of **P2**, **P3** and **P4** were optimized.

During optimization, the product stream was analyzed by FT-IR after reaching steady state (collecting at least 4 mL reaction mixture to the waste). Using optimal conditions, product stream was collected for 20 min (molar amount of substrate is equal to the batch procedure) in steady state operation. The crude mixture was concentrated under reduced pressure and subjected to flash chromatography. *N*-cyclohexylpiperidine-1-carboxamide (**7a**) was obtained as white crystalline solid, 51 mg, 81% yield (for characterization data see below).

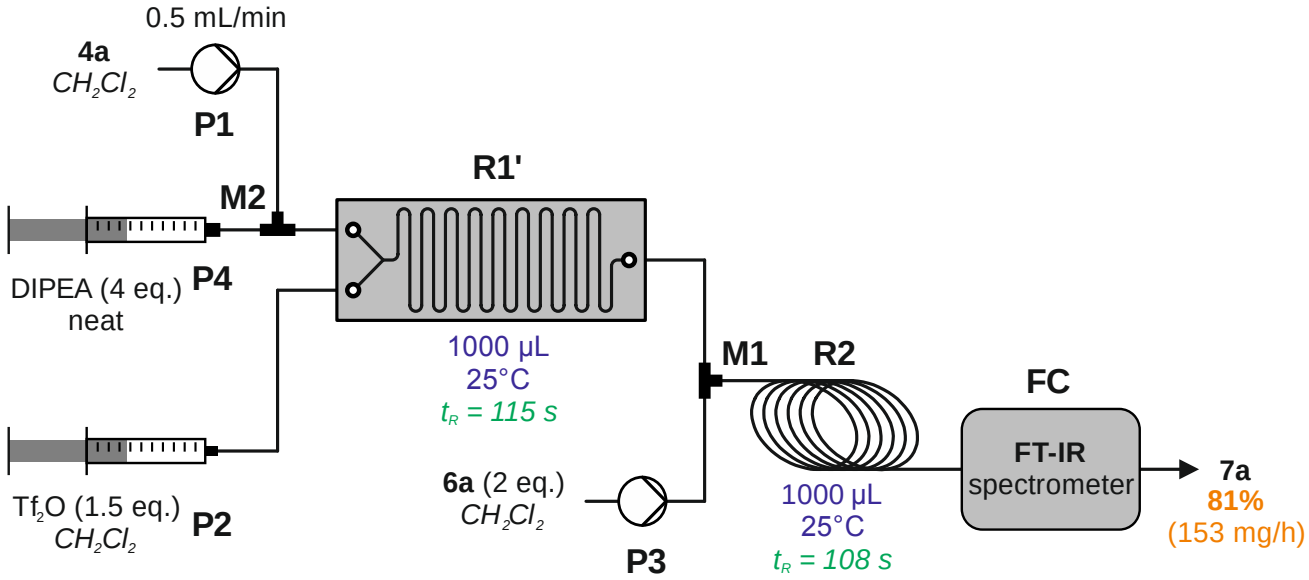


**Fig. S10.** Flow system applying DIPEA, showing optimal settings.

## Detailed parameters of the flow syntheses of ureas 7a-j and 3

**Table S2.** Optimal parameters of the flow synthesis of ureas **7a-j**.
The flow system depicted on Fig. 2 was used as described in the Experimental section. Conversion was 100% for each isolated product.

| *Entry* | *Carbamate (using **P1**)* | *Amine (using **P3**)* | $\dot{V}$(**P1**) *[mL/min]* | $\dot{V}$(**P2**) *[µL/min]* | $\dot{V}$(**P3**) *[mL/min]* | $t_{R1}$ *[s]* | $t_{R2}$ *[s]* | *Product* | *Isolated yield [%]* |
|---|---|---|---|---|---|---|---|---|---|
| *1* | **4a** | **6a** | 0.5 | 16.5 (1.1 eq.) | 0.222 (4 eq.) | 33 | 93 | **7a** | 97 (91 [a]) |
| *2* | **4a** | **6b** | 0.5 | 16.5 | 0.194 (3.5 eq.) | 33 | 97 | **7b** | 88 |
| *3* | **4a** | **6c** | 0.5 | 16.5 | 0.389 (7 eq.) | 33 | 76 | **7c** | 79 |
| *4* | **4a** | **6d** · HCl | 0.5 | 16.5 | 0.250 (1.5 eq.)[b] | 33 | 90 | **7d** | 83 |
| *5* | **4a** | **6e** | 0.5 | 16.5 | 0.5 (9 eq.) | 33 | 68 | **7e** | 74 (35 [a]) |
| *6* | **4b** | **6a** | 0.5 | 16.5 | 0.222 (4 eq.) | 33 | 93 | **7f** | 64 |
| *7* | **4b** | **6b** | 0.5 | 16.5 | 0.194 (3.5 eq.) | 33 | 97 | **7g** | 78 |
| *8* | **4b** | **6c** | 0.5 | 16.5 | 0.250 (4.5 eq.) | 33 | 90 | **7h** | 87 |
| *9* | **4b** | **6d** · HCl | 0.5 | 16.5 | 0.250 (1.5 eq.)[b] | 33 | 90 | **7i** | 86 |
| *10* | **4b** | **6e** | 0.5 | 16.5 | 0.5 (9 eq.) | 33 | 68 | **7j** | –[c] (83 [a]) |
| *11* | **8** | **6d** · HCl | 0.5 | 27 (1.8 eq.) | 0.333 (2 eq.)[d] | 31 | 81 | **3** | 76 |
| *12* | **8** | **6d** · HCl | 0.5 | 27 (1.8 eq.) | 0.273 (5 eq.)[e] | 31 | 87 | **3** | 83 |

[a] Yield of the batch reactions. General conditions: carbamate (1 eq.), $Tf_2O$ (1.5 eq.), 2-chloropyridine (3 eq.), amine (9 eq.); 25 °C; 50 min, then 20 h.

[b] Concentration of **6d** · HCl was 0.09 M and 4.5 eq. of TEA (0.27 M) was used.

[c] The product was not isolated, due to low conversion.

[d] Concentration of **6d** · HCl was 0.09 M and 6 eq. of TEA (0.27 M) was used.

[e] Concentration of **6d** · HCl was 0.27 M and solid $K_3PO_4$ was used to solubilize dimethylamine.

## Characterization data of known compounds

Melting points were determined using EZ-Melt MPA120 (Stanford Research Systems, Sunnyvale, CA, USA) apparatus and were uncorrected.

FT-IR spectra of the purified products were measured using Bruker ALPHA FT-IR spectrometer (Bruker Optik GmbH., Ettlingen, Germany) equipped with Harrick TFC-S13-3 flow cell (Harrick Scientific Products Inc., Pleasantville, NY, USA) using 100 μm optical path and ZnSe windows. The samples were introduced as a dichloromethane solution, 16 scans were recorded and the background of the pure solvent was subtracted.

NMR spectra were recorded at 25 °C on an Agilent (Varian) NMRS-500 spectrometer at 500 MHz for $^{1}$H and 126 MHz for $^{13}$C using DMSO-$d_6$ as solvent (unless otherwise stated). The chemical shifts (δ) were referenced to tetramethylsilane (TMS). Electrospray high-resolution MS measurements (ESI-HRMS) were performed on a Thermo LTQ FT Ultra spectrometer (Thermo Fisher Scientific, Bremen, Germany). The ionization method was ESI and operated in positive ion mode, the ion transfer capillary temperature was set at 280 °C. Samples were infused into the ESI source MeOH solutions at a flow rate of 10 μL/min. Resolving power of 50,000 (FWHM) at *m/z* 400. Data acquisition and analysis were accomplished with Xcalibur software version 2.1 (Thermo Fisher Scientific Inc.). Electron impact high-resolution MS measurements (EI-HRMS) were performed on a Finnigan MAT 95XP mass spectrometer (Finnigan, Bremen, Germany). The ion source temperature was set at 220 °C, the applied ionization energy was 70 eV. Data acquisition and analysis were accomplished with Xcalibur software version 2.0 (Thermo Fisher Scientific Inc.).

*N-Cyclohexylpiperidine-1-carboxamide (**7a**)*

**Melting point:** 140.2 – 141.4 ºC (lit. 140 – 141 ºC)[S1]

**IR** (6.3 mg/mL): $\nu_{max}$ 3460, 2937, 2856, 1640, 1510, 1451 cm$^{-1}$;

**$^{1}$H NMR**: δ 6.00 (br d, *J* = 7.7 Hz, 1H), 3.37 (tdt, *J* = 11.0, 7.6, 3.9 Hz, 1H), 3.25 – 3.19 (m, 4H), 1.77 – 1.68 (m, 2H), 1.68 – 1.61 (m, 2H), 1.59 – 1.52 (m, 1H), 1.52 – 1.46 (m, 2H), 1.42 – 1.34 (m, 4H), 1.26 – 1.18 (m, 2H), 1.18 – 1.09 (m, 2H), 1.05 (qt, *J* = 12.1, 3.3 Hz, 1H) ppm;

**$^{13}$C NMR**: δ 156.7, 49.1, 44.3, 33.2, 25.4, 25.3, 25.1, 24.2 ppm;

**ESI-HRMS:** calcd for $C_{12}H_{23}ON_2$ $[M+H]^+$: 211.18049; found: 211.18067; delta=0.8 ppm.

Spectral data are consistent with literature.[S2]

*N-Cyclohexylpyrrolidine-1-carboxamide (**7b**)*

**Melting point:** 138.4 – 139.7 ºC

**IR** (6 mg/mL): $\nu_{max}$ 3446, 2934, 2857, 1642, 1515 $cm^{-1}$;

**$^{1}$H NMR**: δ 5.62 (br d, *J* = 7.9 Hz, 1H), 3.37 (tdt, *J* = 11.1, 7.9, 3.7 Hz, 1H), 3.21 – 3.11 (m, 4H), 1.79 – 1.74 (m, 4H), 1.75 – 1.70 (m, 2H), 1.70 – 1.62 (m, 2H), 1.60 – 1.51 (m, 1H), 1.28 – 1.19 (m, 2H), 1.19 – 1.11 (m, 2H), 1.05 (qt, *J* = 12.2, 3.4 Hz, 1H) ppm;

**$^{13}$C NMR**: δ 155.8, 48.7, 45.2, 33.3, 25.4, 25.1, 25.0 ppm;

**ESI-HRMS:** calcd for $C_{11}H_{21}ON_2$ $[M+H]^+$: 197.16484; found: 197.16503; delta=0.9 ppm.

Spectral data are consistent with literature.[S3]

*N-Cyclohexylmorpholine-4-carboxamide (**7c**)*

**Melting point:** 179.6 – 180.3 ºC (lit. 163 – 168 ºC)[S4]

**IR** (6.3 mg/mL): $\nu_{max}$ 3458, 2934, 2857, 1650, 1511, 1452, 1119 $cm^{-1}$;

**$^{1}$H NMR**: δ 6.15 (br d, *J* = 7.7 Hz, 1H), 3.56 – 3.48 (m, 4H), 3.39 (tdt, *J* = 11.0, 7.4, 3.8 Hz, 1H), 3.26 – 3.15 (m, 4H), 1.80 – 1.70 (m, 2H), 1.70 – 1.62 (m, 2H), 1.60 – 1.51 (m, 1H), 1.28 – 1.19 (m, 2H), 1.20 – 1.10 (m, 2H), 1.06 (qt, *J* = 12.4, 3.3 Hz, 1H) ppm;

**$^{13}$C NMR**: δ 157.0, 65.9, 49.1, 43.9, 33.1, 25.3, 25.1 ppm;

**ESI-HRMS:** calcd for $C_{11}H_{21}O_2N_2$ $[M+H]^+$: 213.15975; found: 213.15989; delta=0.6 ppm.

Spectral data are consistent with literature.[S4]

*3-Cyclohexyl-1,1-dimethylurea (**7d**)*

**Melting point:** 155.9 – 157.2 ºC (lit. 154 – 155 ºC)[S5]

**IR** (5 mg/mL): $\nu_{max}$ 3457, 2934, 2856, 1650, 1516, 1354 $cm^{-1}$;

**$^{1}$H NMR**: δ 5.83 (br d, *J* = 7.7 Hz, 1H), 3.36 (tdt, *J* = 11.3, 7.2, 3.8 Hz, 1H), 2.75 (s, 6H), 1.78 – 1.69 (m, 2H), 1.69 – 1.61 (m, 2H), 1.60 – 1.51 (m, 1H), 1.27 – 1.19 (m, 2H), 1.20 – 1.10 (m, 2H), 1.06 (qt, *J* = 12.5, 3.4 Hz, 1H) ppm;

**$^{13}$C NMR**: δ 157.5, 49.1, 35.9, 33.2, 25.4, 25.1 ppm;

**ESI-HRMS:** calcd for $C_9H_{19}ON_2$ $[M+H]^+$: 171.14919; found: 171.14930; delta=0.6 ppm.

Spectral data are consistent with literature.[S5]

*3-Cyclohexyl-1,1-diisopropylurea (**7e**)*

**Melting point:** 97.1 – 97.9ºC (lit. 99 – 100 ºC)[S2]

**IR** (6.7 mg/mL): $\nu_{max}$ 3481, 2934, 2856, 1632, 1508 $cm^{-1}$;

**$^1$H NMR**: δ 5.42 (br d, *J* = 7.7 Hz, 1H), 3.67 (hept, *J* = 6.7 Hz, 2H), 3.47 – 3.34 (m, 1H), 1.75 – 1.69 (m, 2H), 1.69 – 1.62 (m, 2H), 1.59 – 1.51 (m, 1H), 1.28 – 1.20 (m, 2H), 1.20 – 1.16 (m, 2H), 1.14 (d, *J* = 6.6 Hz, 12H), 1.11 – 0.97 (m, 1H) ppm;

**$^{13}$C NMR**: δ 155.7, 48.7, 44.6, 33.2, 25.4, 25.2, 21.3 ppm;

**ESI-HRMS:** calcd for $C_{13}H_{27}ON_2$ $[M+H]^+$: 227.21179; found: 227.21210; delta=1.3 ppm.

Spectral data are consistent with literature.[S2]

*Ethyl 2-(*trans*-4-(3,3-dimethylureido)cyclohexyl)acetate (**7i**)*

**Melting point:** 101.7 – 104.2 ºC

**IR** (7.7 mg/mL): $\nu_{max}$ 3457, 2932, 2854, 1727, 1647, 1517, 1355 $cm^{-1}$;

**$^1$H NMR**: δ 5.85 (d, *J* = 7.9 Hz, 1H), 4.04 (q, *J* = 7.0 Hz, 2H), 3.33 (tdt, *J* = 12.0, 7.9, 3.7 Hz, 1H), 2.74 (s, 6H), 2.17 (d, *J* = 7.0 Hz, 2H), 1.78 – 1.71 (m, 2H), 1.70 – 1.64 (m, 2H), 1.62 – 1.52 (m, 1H), 1.25 – 1.14 (m, 2H), 1.17 (t, *J* = 7.1 Hz, 3H), 1.05 – 0.94 (m, 2H) ppm;

**$^{13}$C NMR**: δ 172.1, 157.5, 59.6, 49.0, 40.8, 35.8, 33.9, 32.6, 31.3, 14.1 ppm;

**EI-HRMS:** calcd for $C_{13}H_{24}O_3N_2$ $[M]^+$: 256.17814; found: 256.17872; delta=2.2 ppm.

Spectral data are consistent with literature.[S6]

*Cariprazine (**3**)*

**Melting point:** 208.3 – 210.3 ºC (lit. 208 – 211 ºC)[S7,S8]

**IR** (13 mg/mL): $\nu_{max}$ 3457, 3044, 2930, 2852, 2824, 1647, 1517, 1355 $cm^{-1}$;

**$^1$H NMR** (400 MHz, DMSO-$d_6$ + TFA): δ 9.90 (br s, 1H), 7.39 – 7.30 (m, 2H), 7.24 – 7.16 (m, 1H), 3.65 – 3.53 (m, 2H), 3.49 – 3.40 (m, 2H), 3.39 – 3.30 (m, 1H), 3.25 – 3.12 (m, 4H), 3.09 – 2.98 (m, 2H), 2.75 (s, 6H), 1.82 – 1.67 (m, 4H), 1.62 – 1.52 (m, 2H), 1.28 – 1.13 (m, 3H), 1.07 – 0.91 (m, 2H) ppm;

**$^{13}$C NMR** (100 MHz, DMSO-$d_6$ + TFA): δ 157.74, 149.52, 132.87, 128.73, 126.22, 125.46, 119.94, 54.10, 51.32, 49.36, 48.02, 35.95, 34.52, 32.72, 31.57, 30.21 ppm;

**ESI-MS**: [M+H] 427.2.

Spectral data are consistent with literature.[S8–S10] The product was identical with the authentic sample of Cariprazine.

## NMR spectra of the isolated compounds (7a-j, 3)

*N-Cyclohexylpiperidine-1-carboxamide (**7a**) $^{1}H$ and $^{13}C$ NMR (DMSO)*

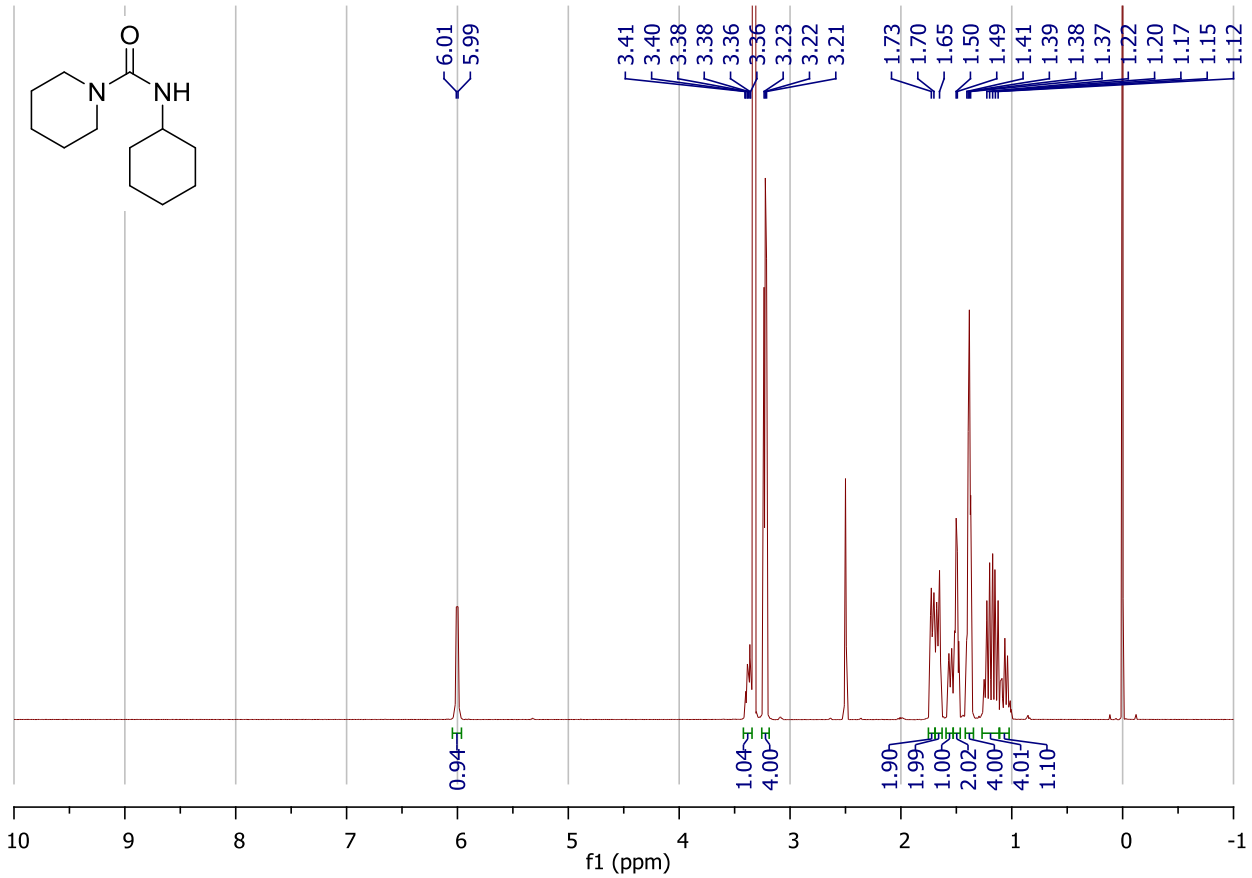


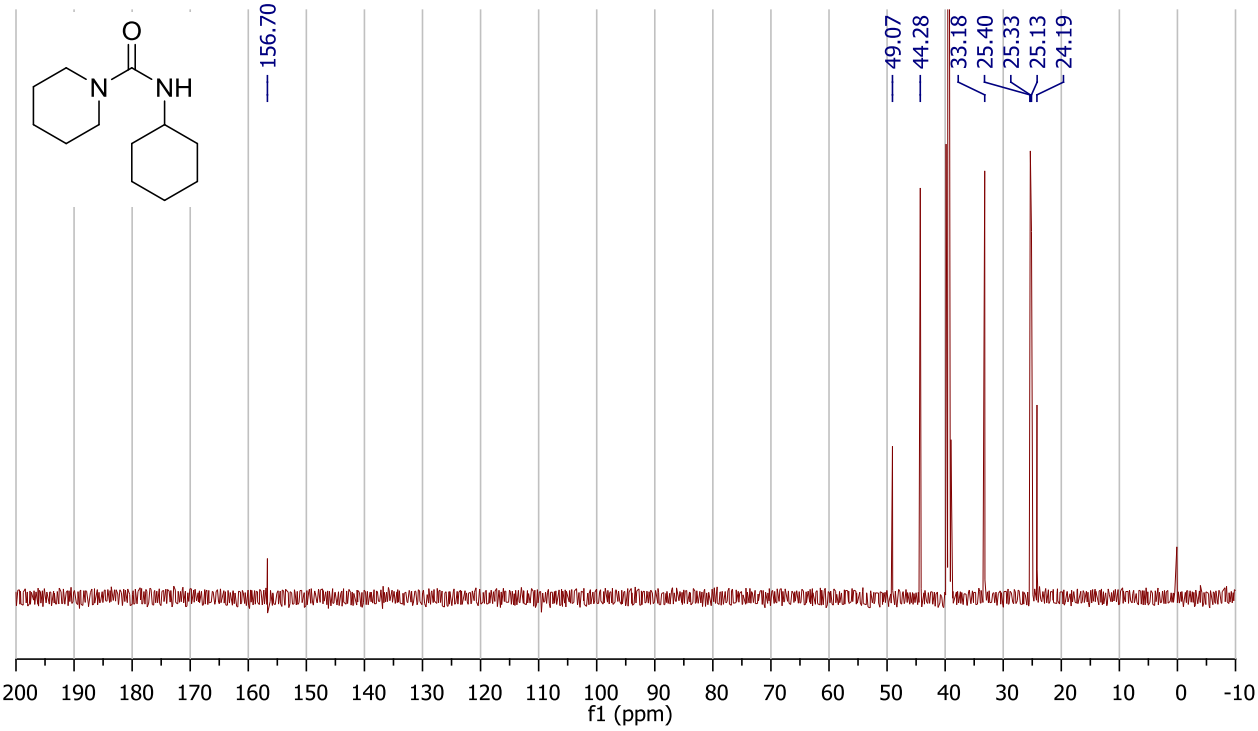

*N-Cyclohexylpyrrolidine-1-carboxamide (**7b**) $^{1}H$ and $^{13}C$ NMR (DMSO)*

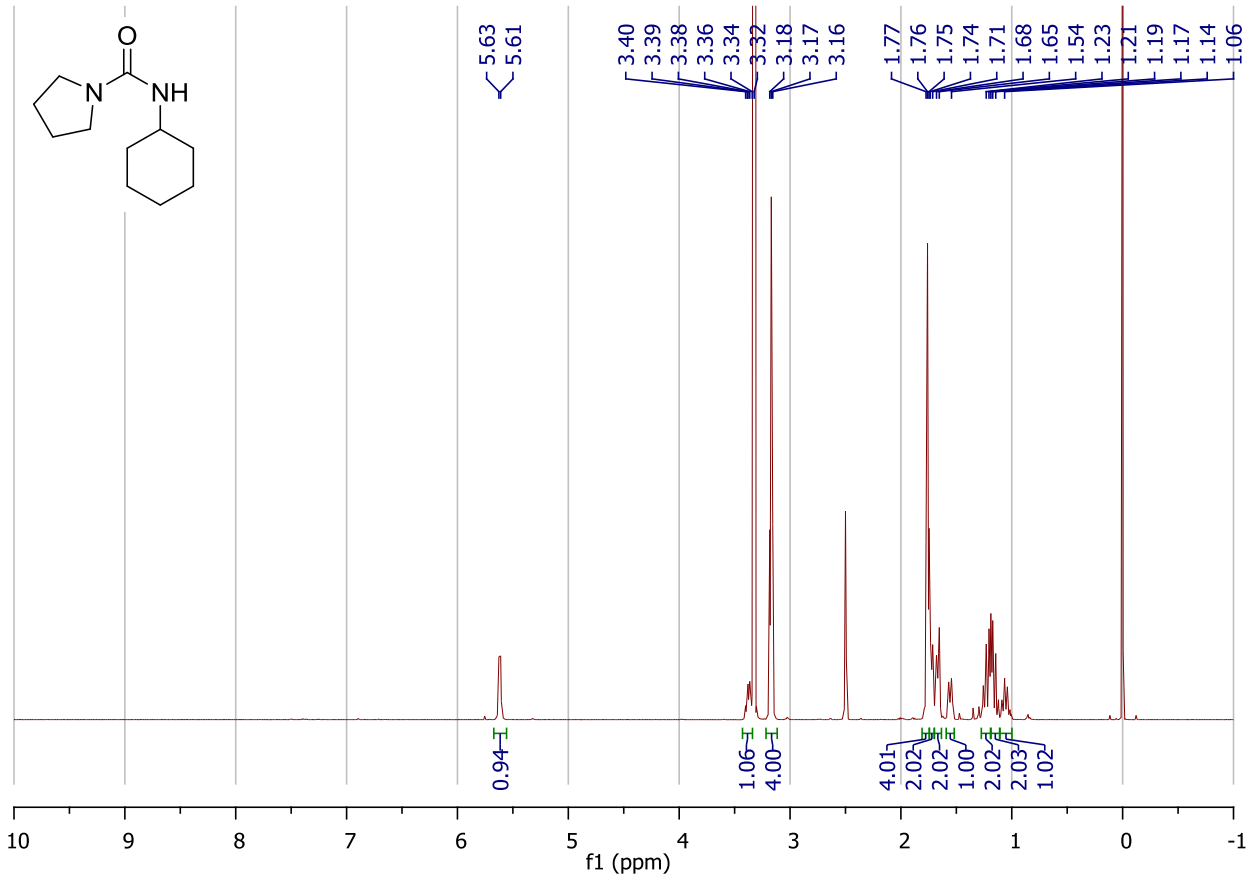


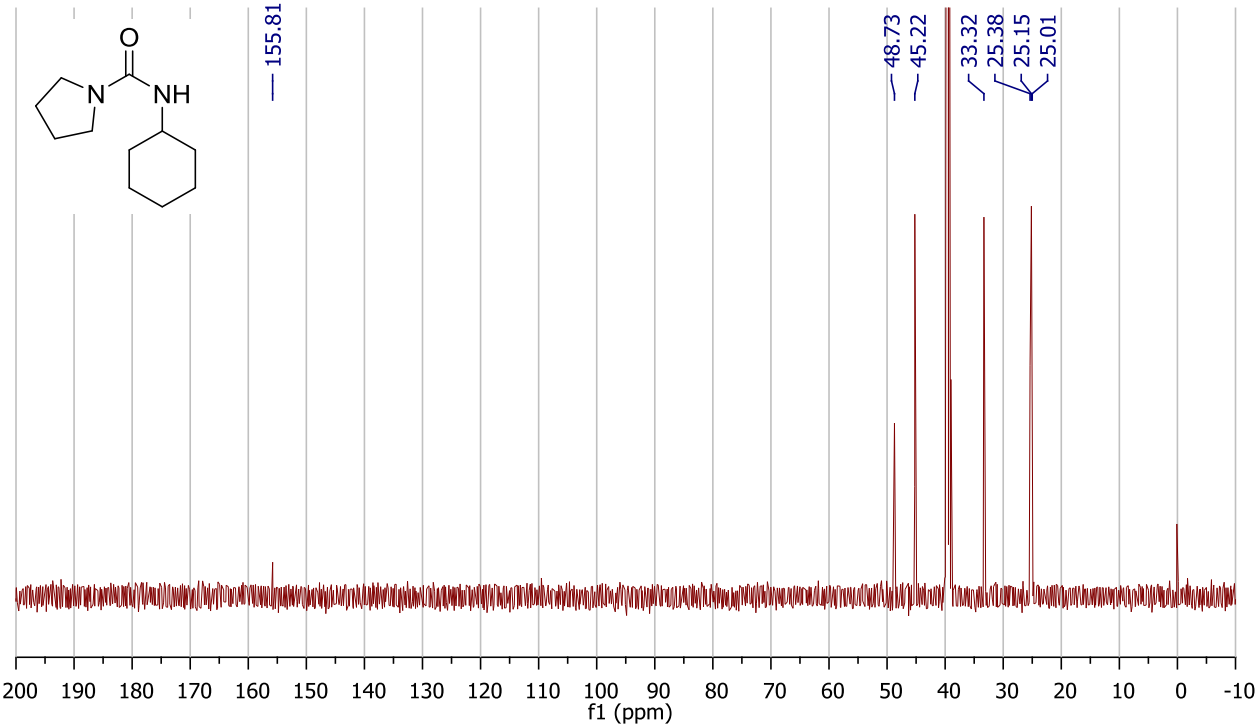

*N-Cyclohexylmorpholine-4-carboxamide (**7c**) $^{1}H$ and $^{13}C$ NMR (DMSO)*

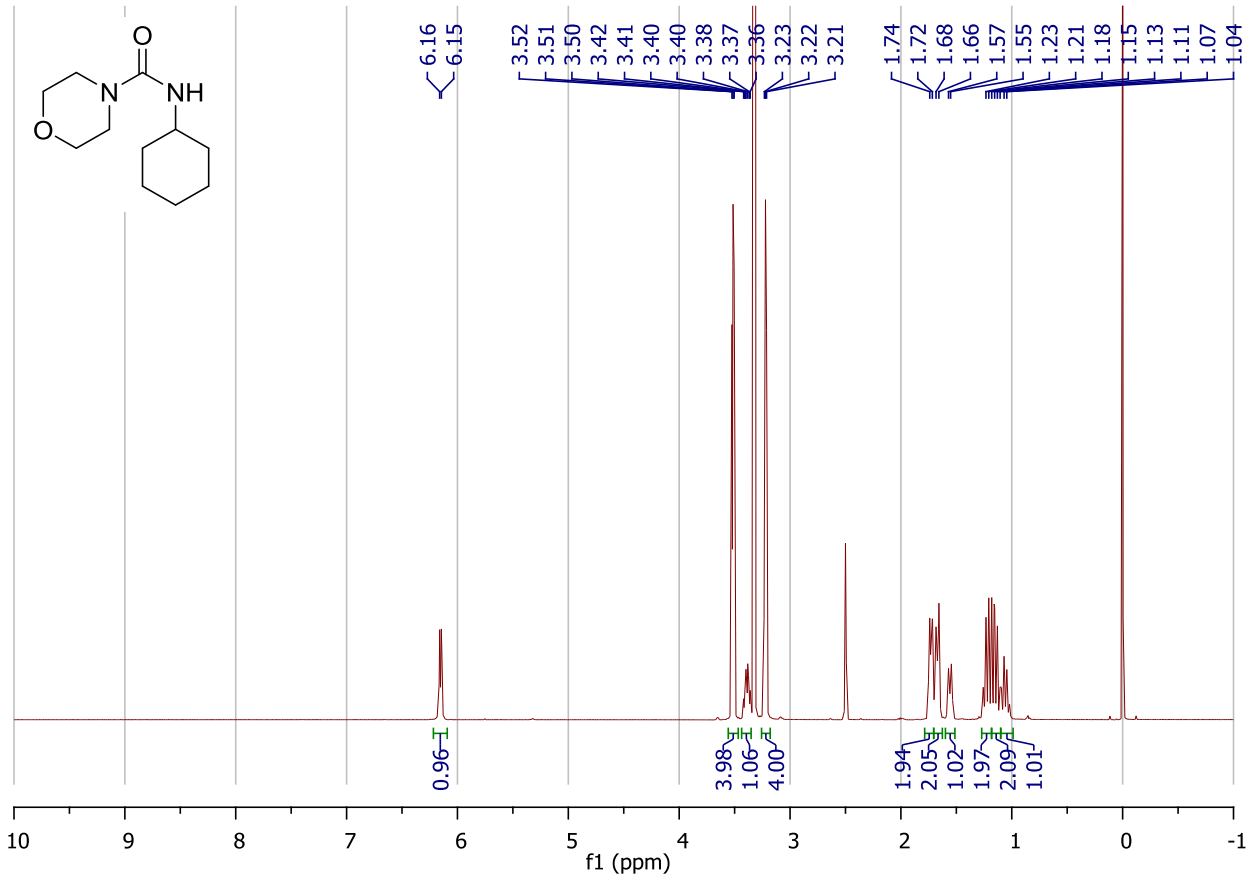


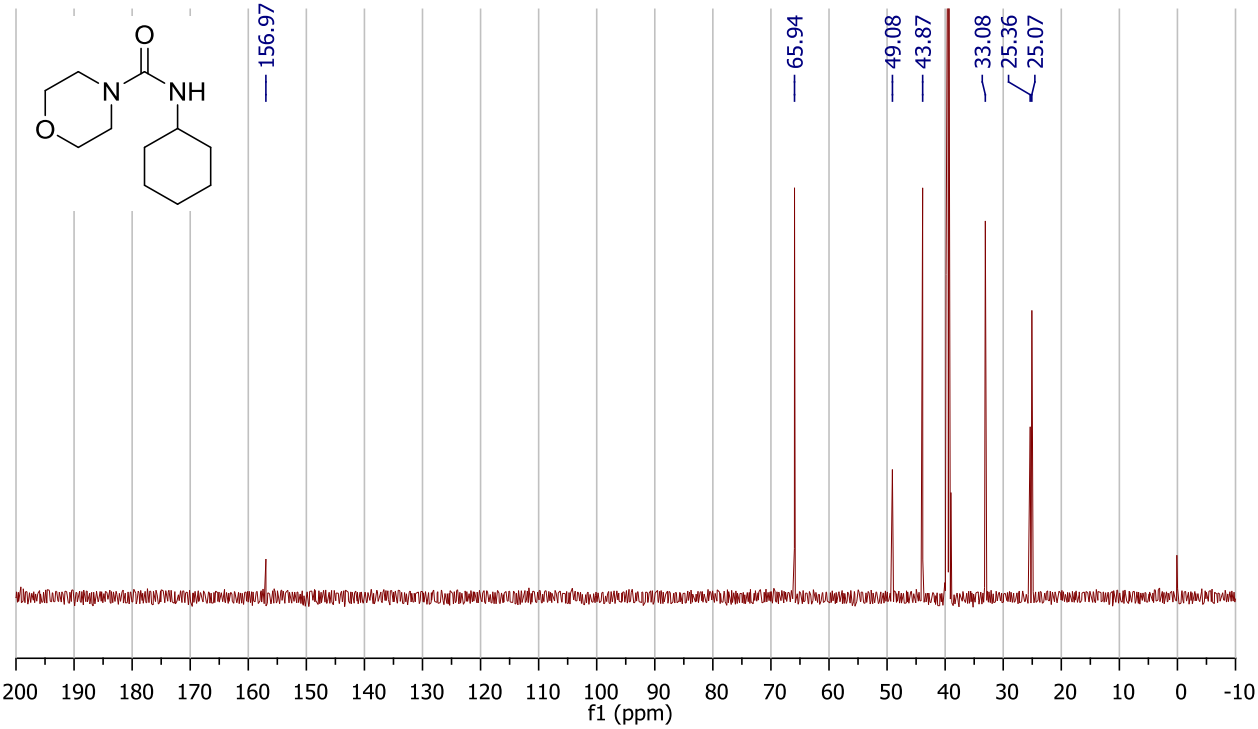

*3-Cyclohexyl-1,1-dimethylurea (**7d**) $^{1}H$ and $^{13}C$ NMR (DMSO)*

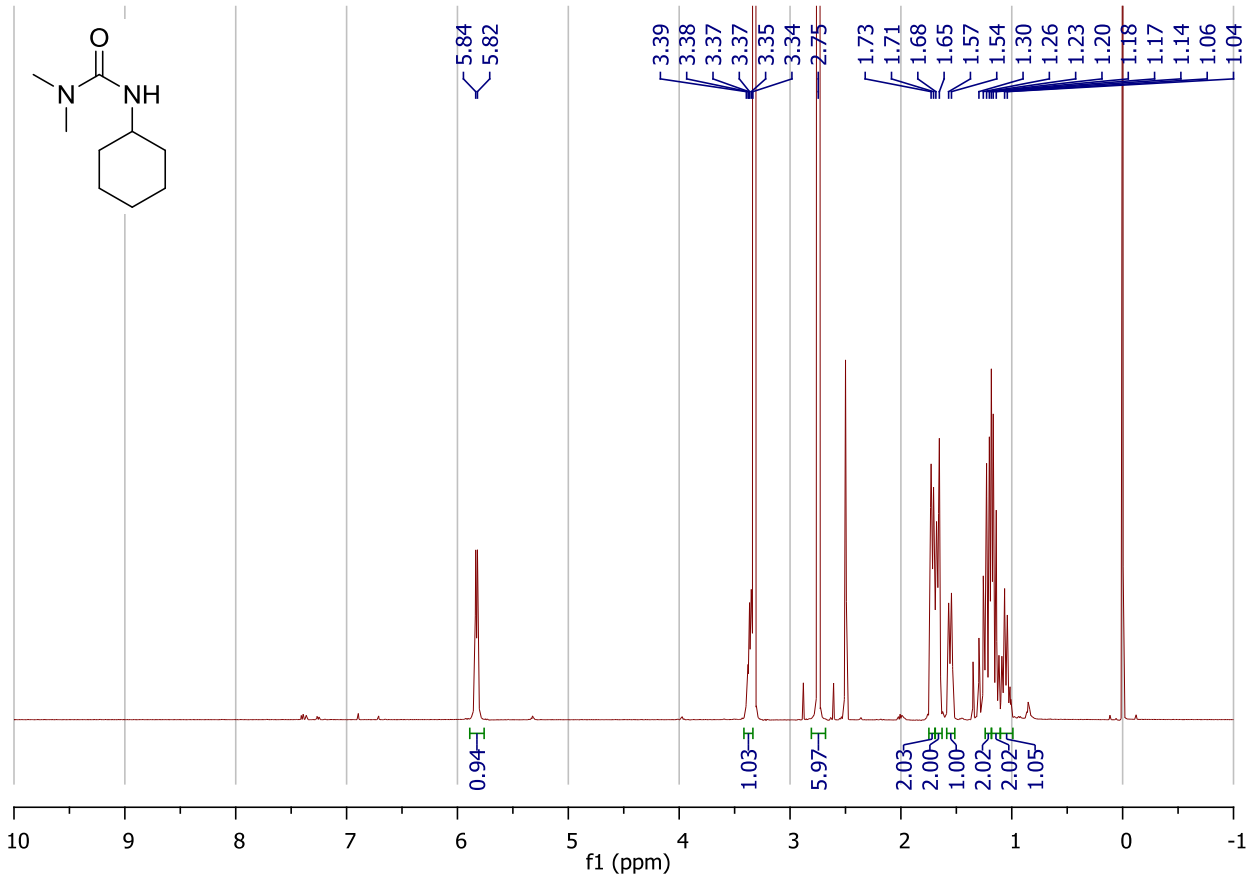


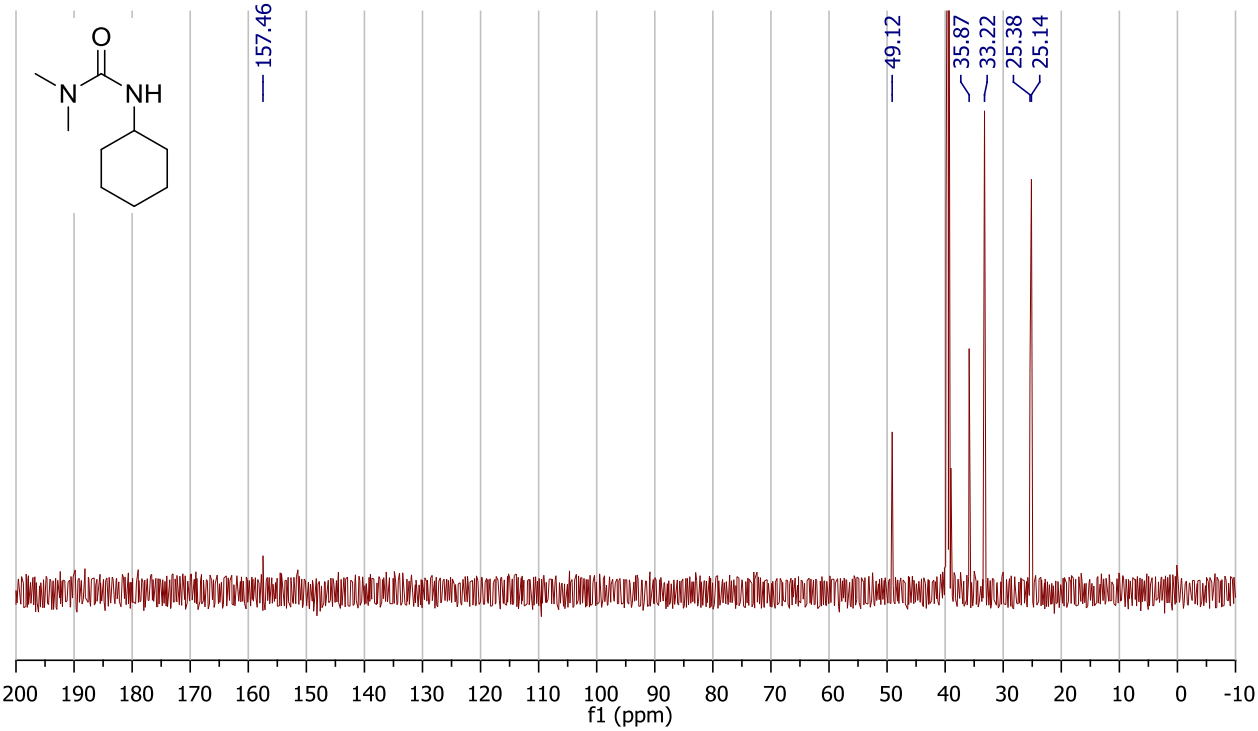

*3-Cyclohexyl-1,1-diisopropylurea (**7e**) $^{1}H$ and $^{13}C$ NMR (DMSO)*

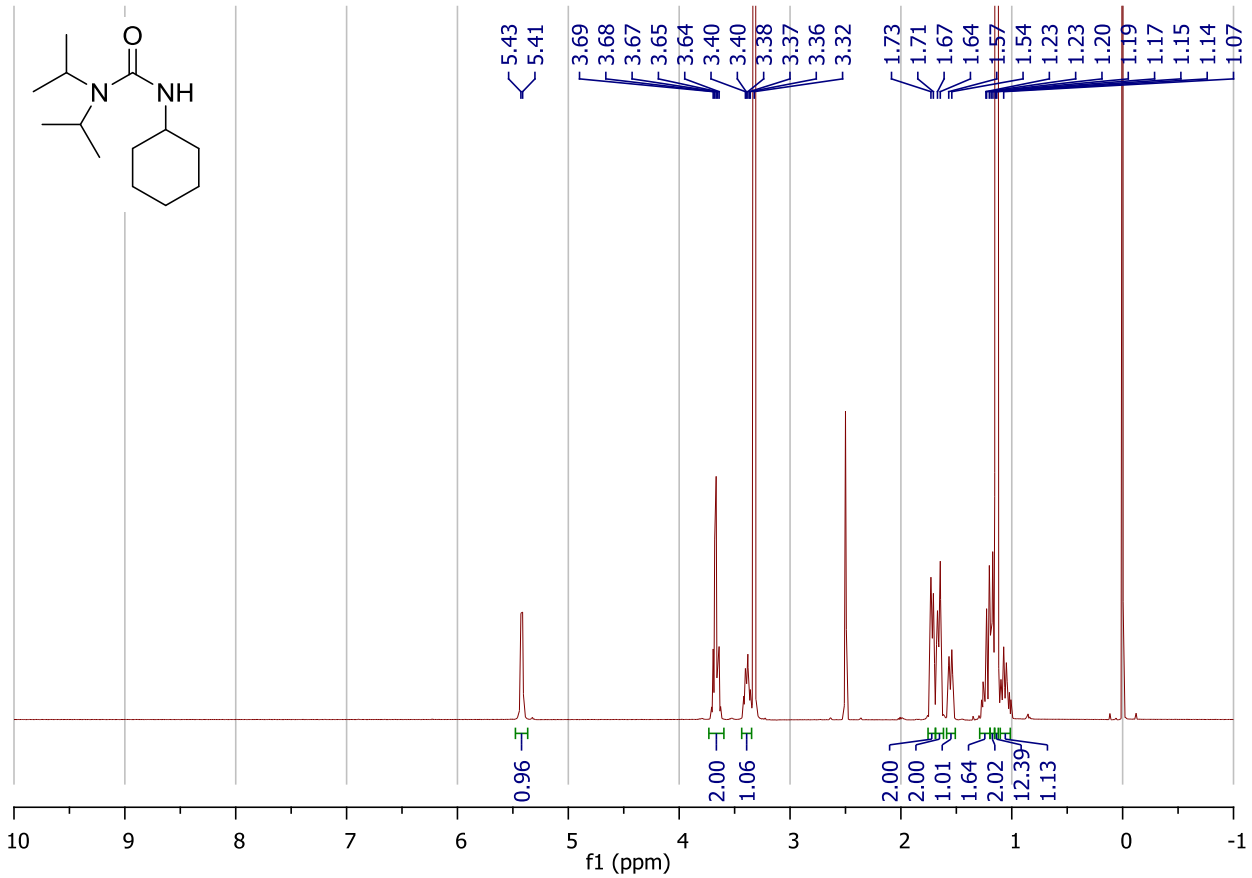


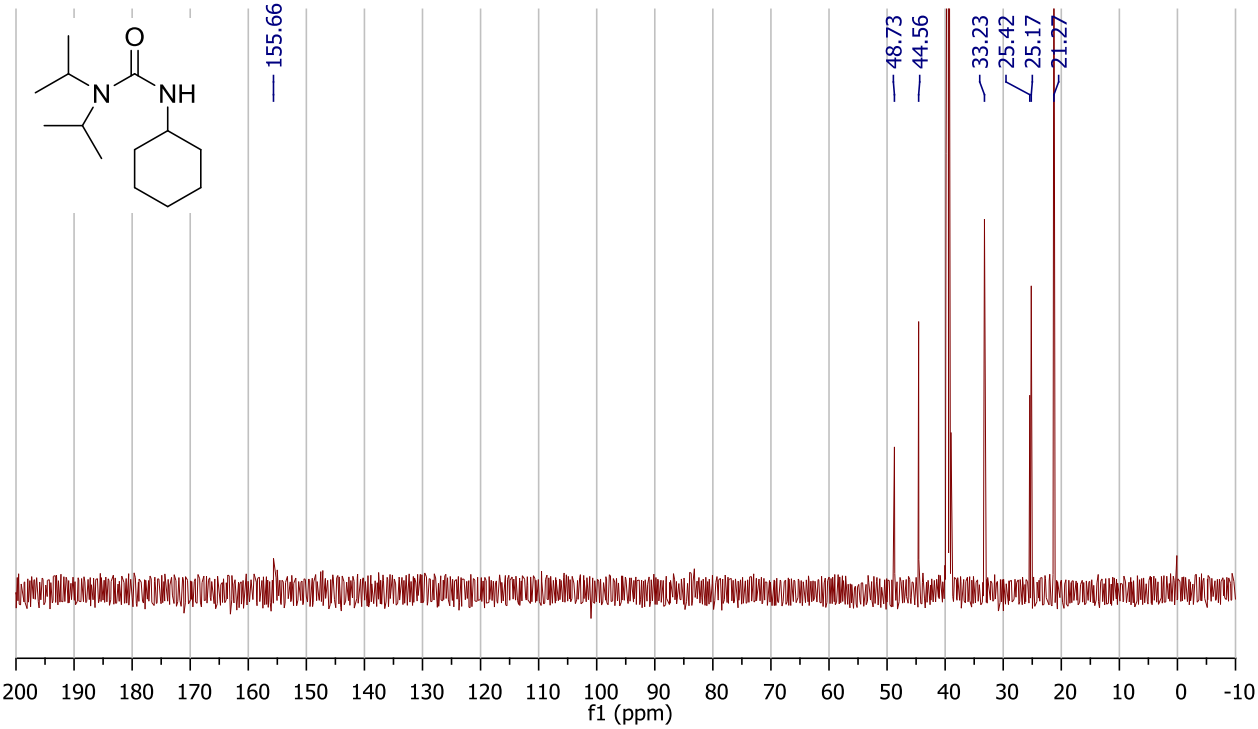

*Ethyl 2-(trans-4-(piperidine-1-carboxamido)cyclohexyl)acetate (**7f**) $^{1}H$ and $^{13}C$ NMR (DMSO)*

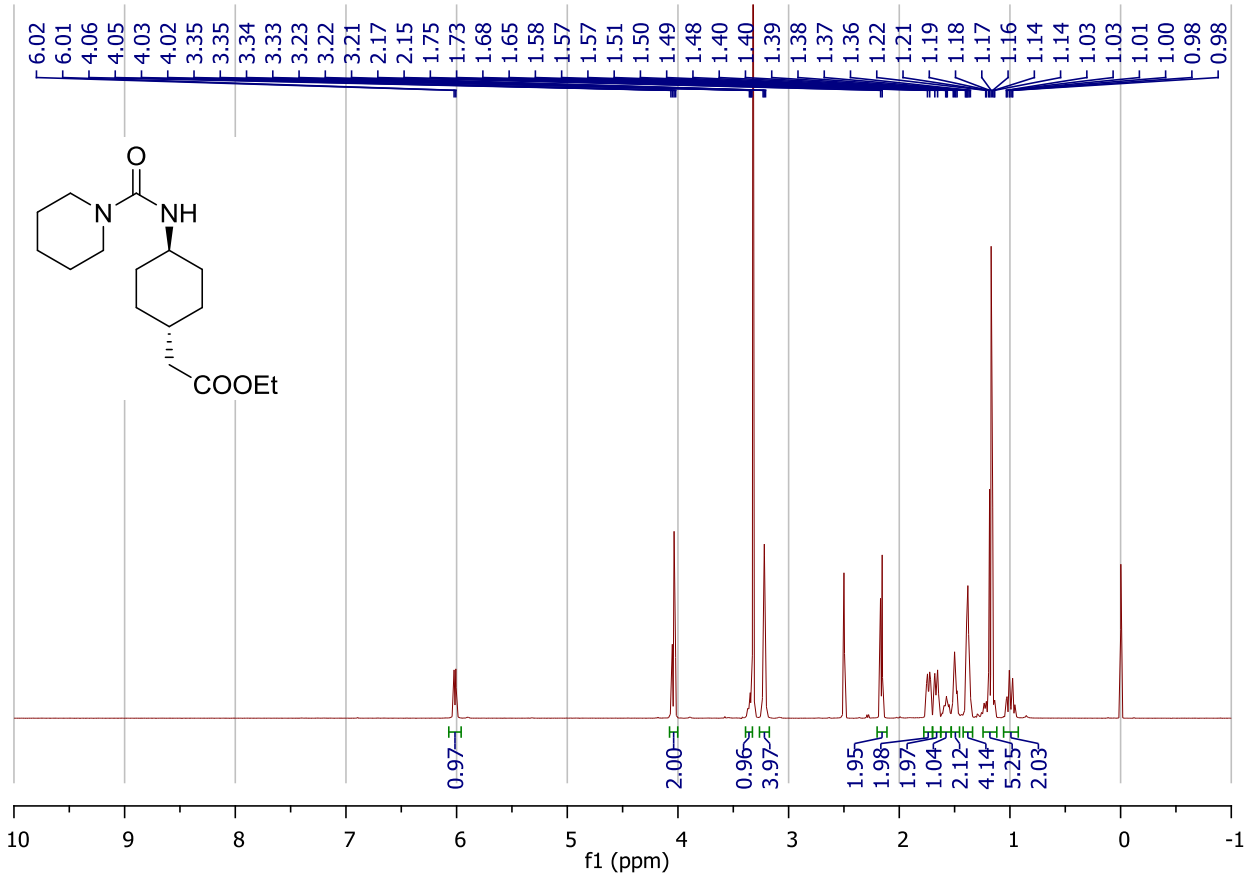


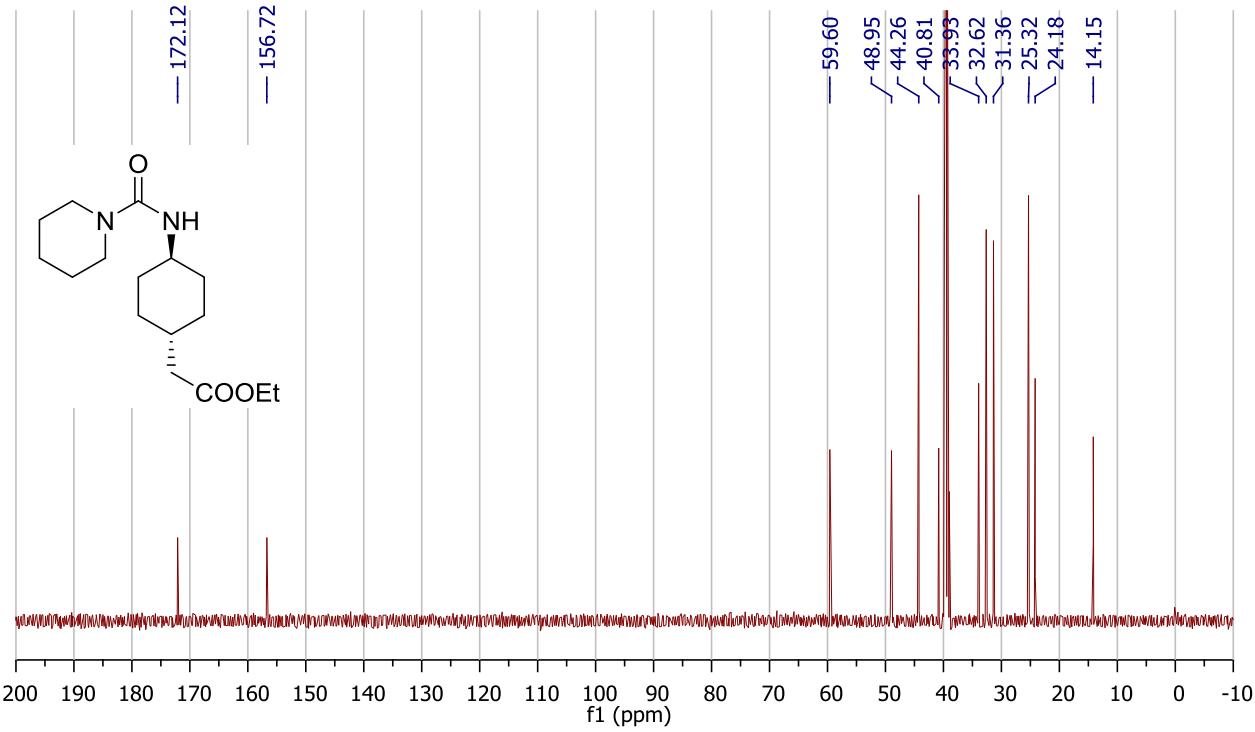

*Ethyl 2-(trans-4-(pyrrolidine-1-carboxamido)cyclohexyl)acetate (**7g**) $^{1}H$ and $^{13}C$ NMR (DMSO)*

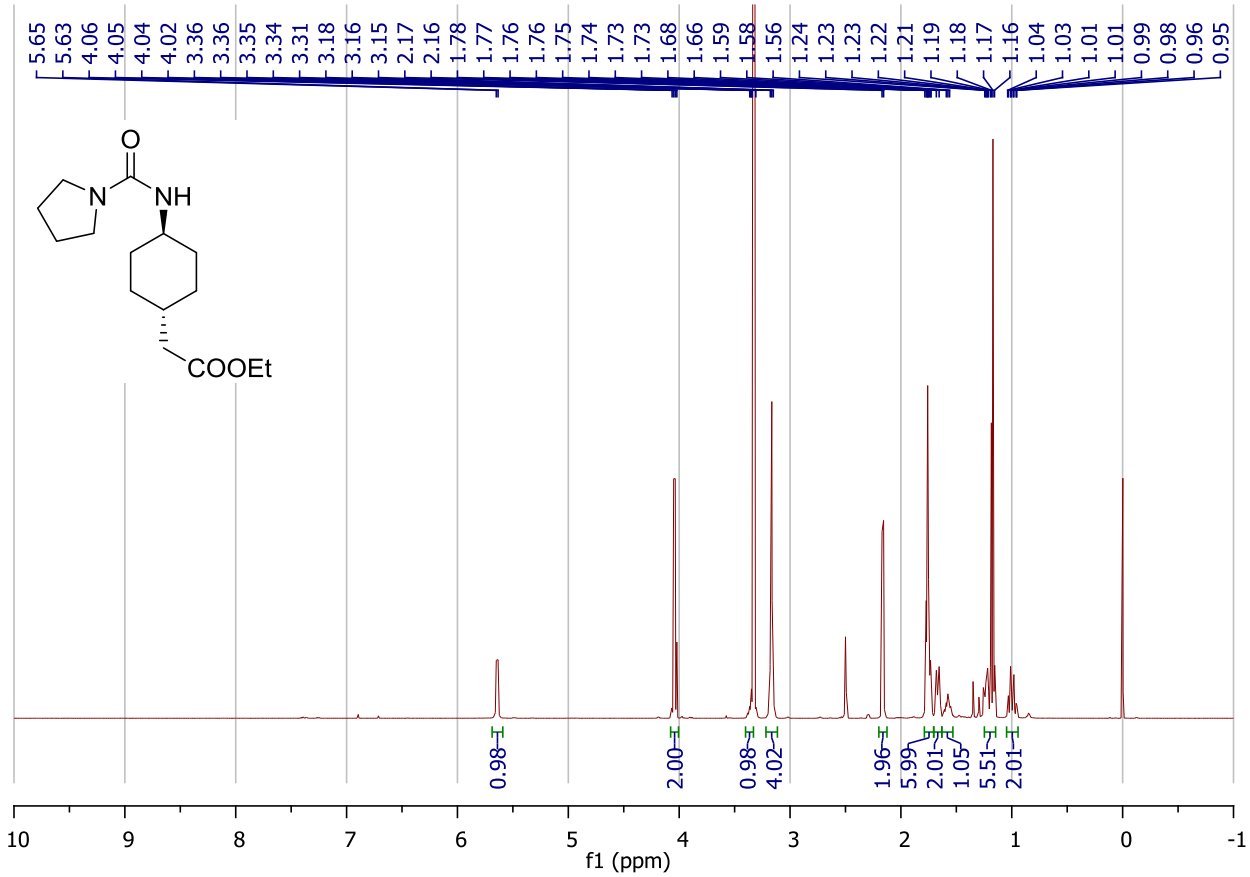


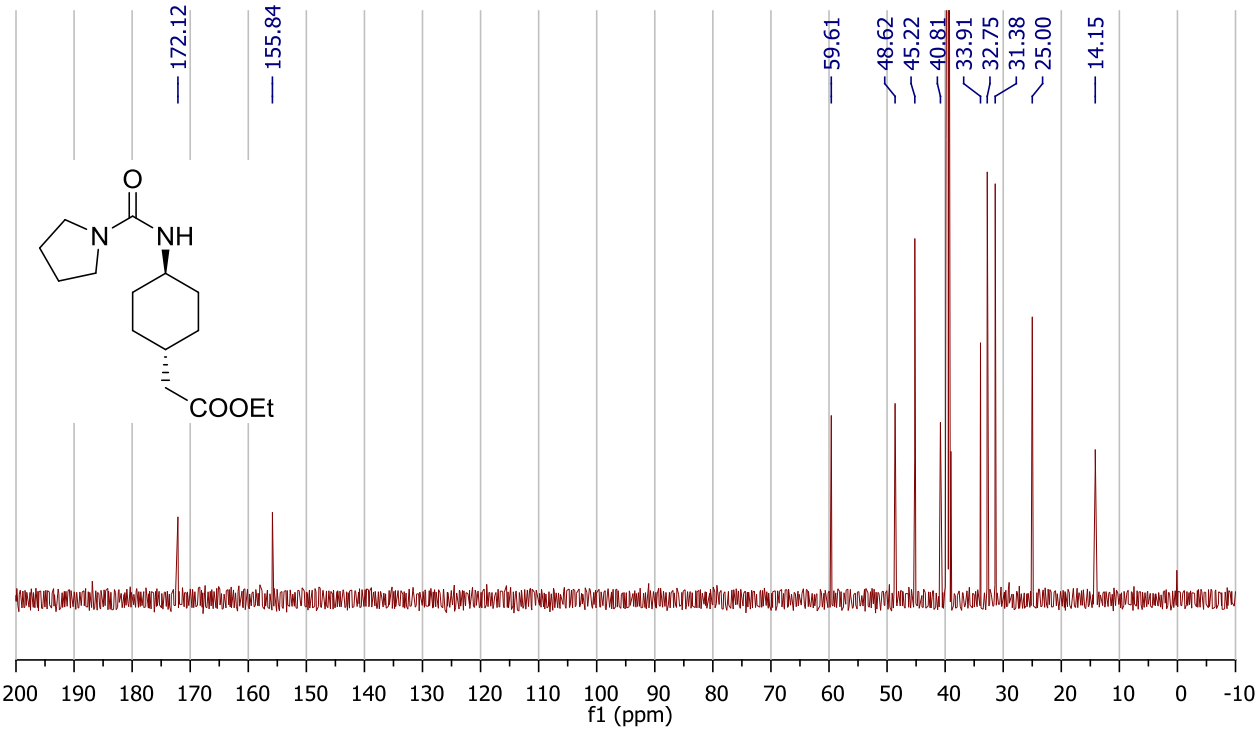

*Ethyl 2-(trans-4-(morpholine-4-carboxamido)cyclohexyl)acetate (**7h**) $^{1}H$ and $^{13}C$ NMR (DMSO)*

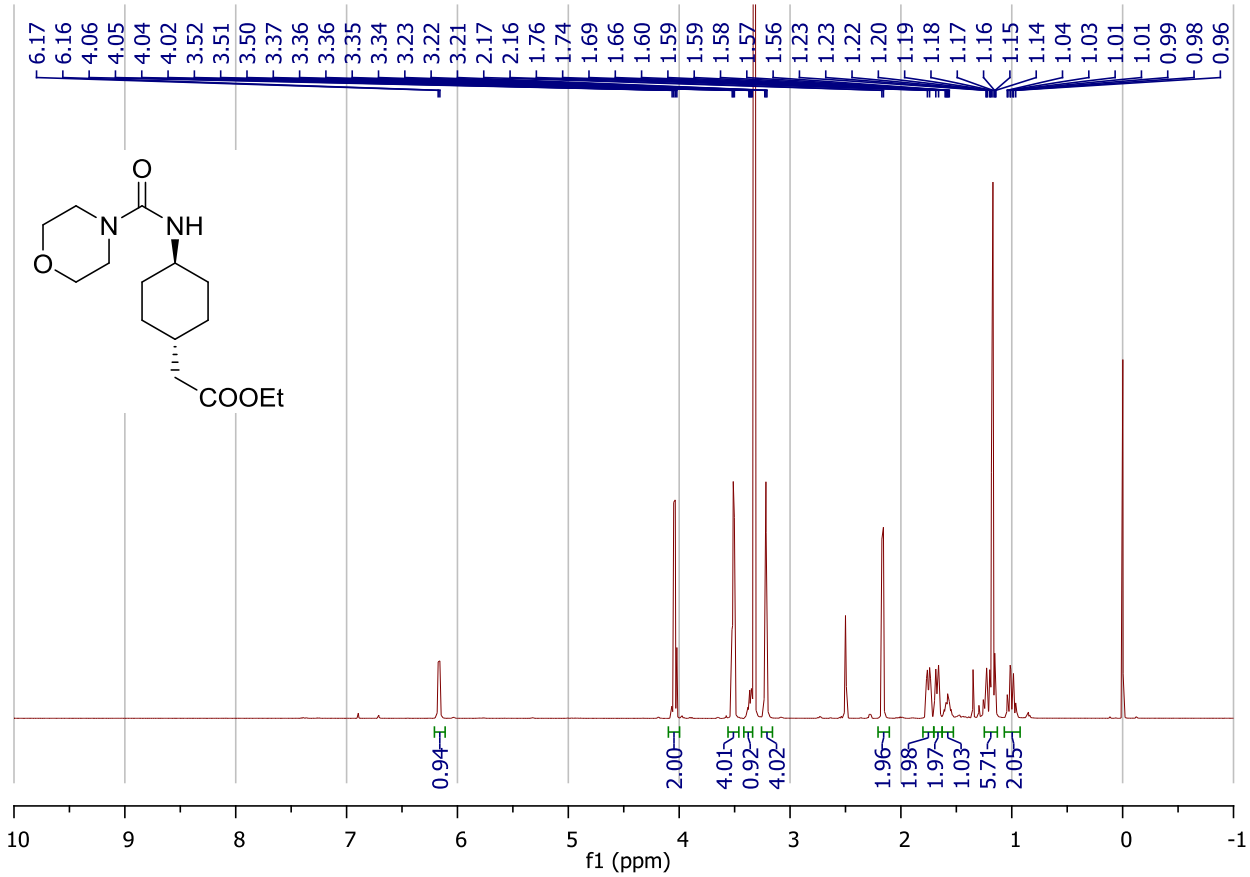


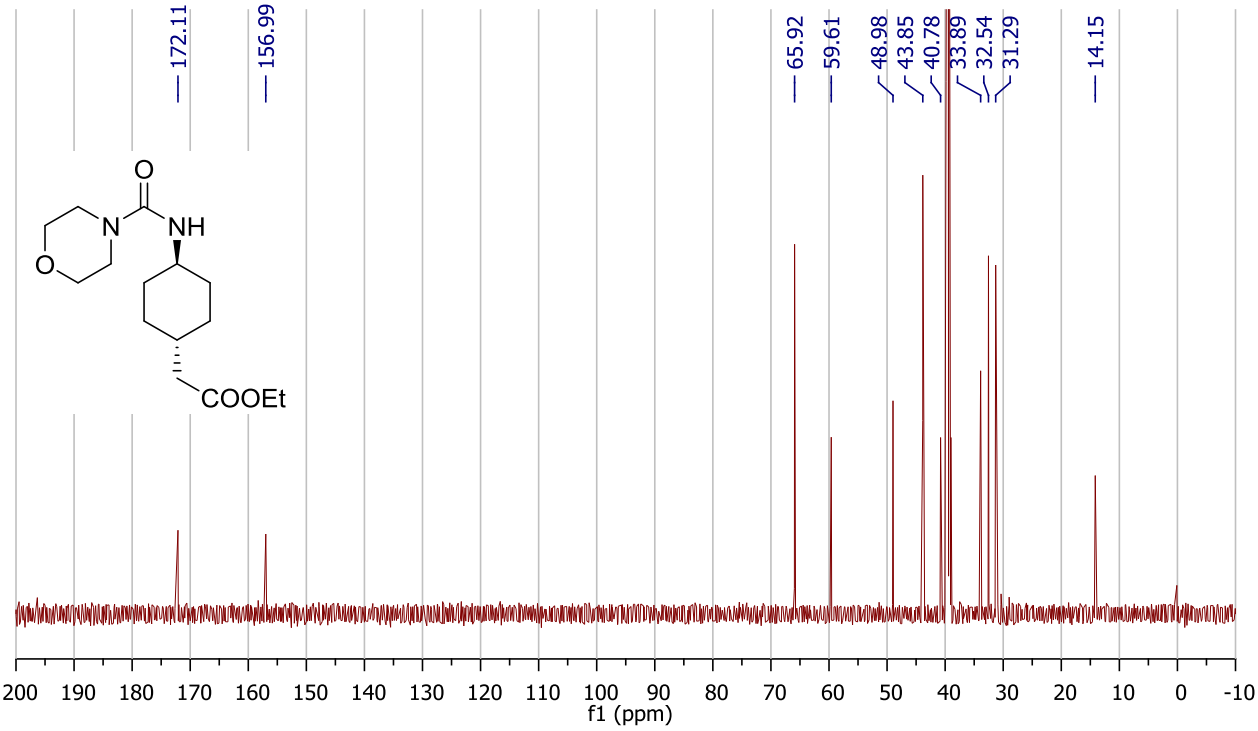

*Ethyl 2-(*trans*-4-(3,3-dimethylureido)cyclohexyl)acetate (**7i**) $^{1}H$ and $^{13}C$ NMR (DMSO)*

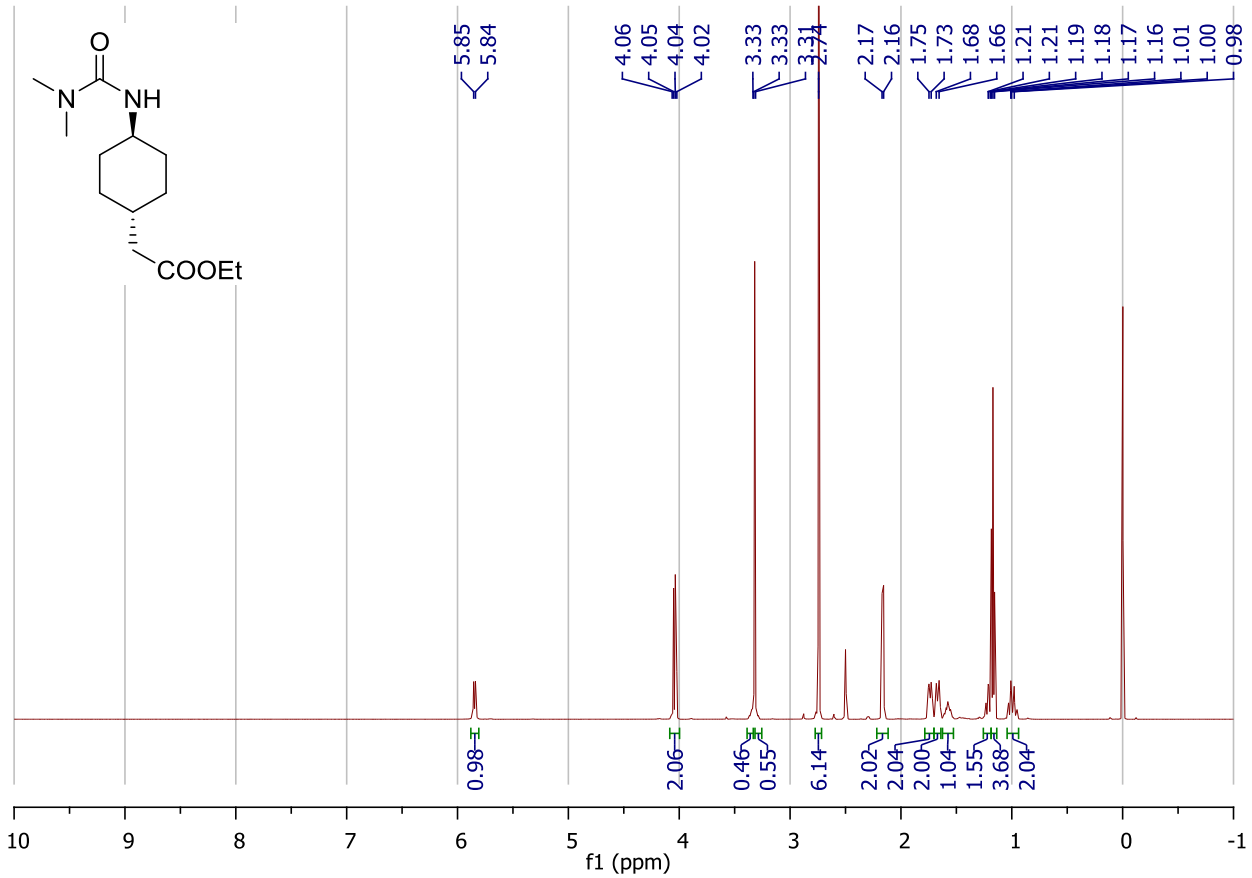


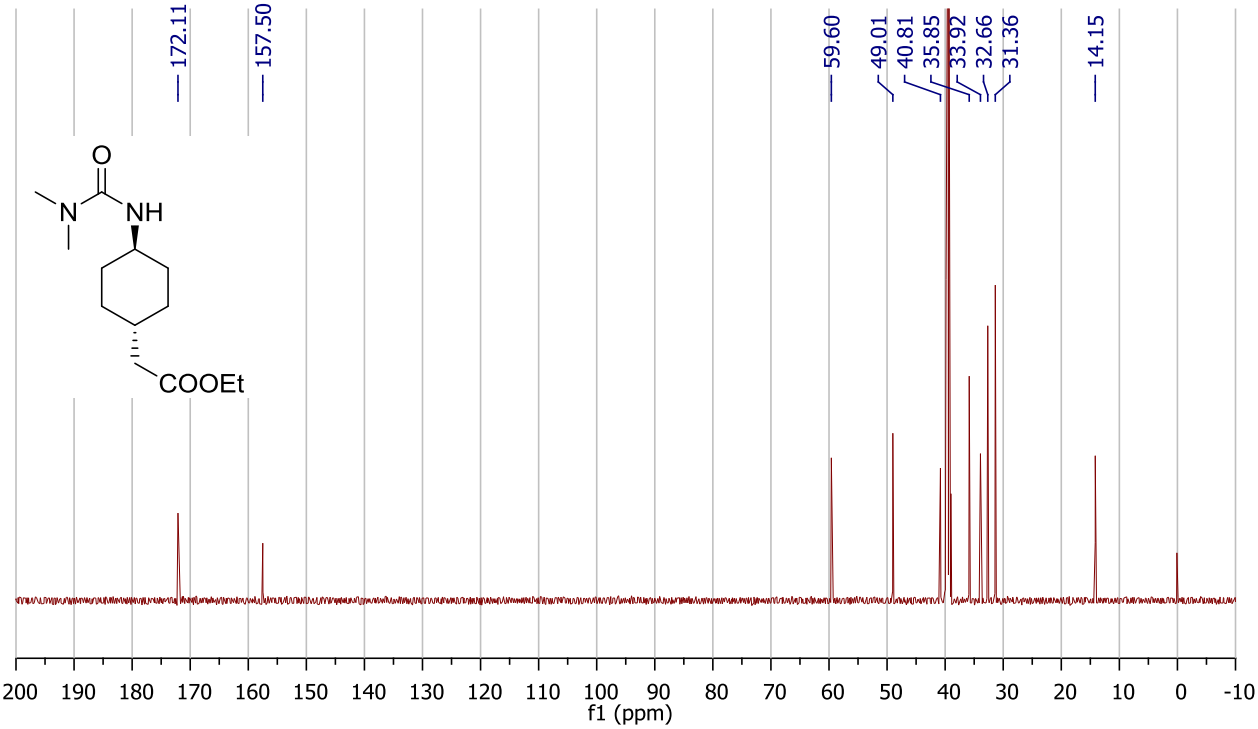

*Ethyl 2-(trans-4-(3,3-diisopropylureido)cyclohexyl)acetate (**7j**) 1H and 13C NMR (DMSO)*

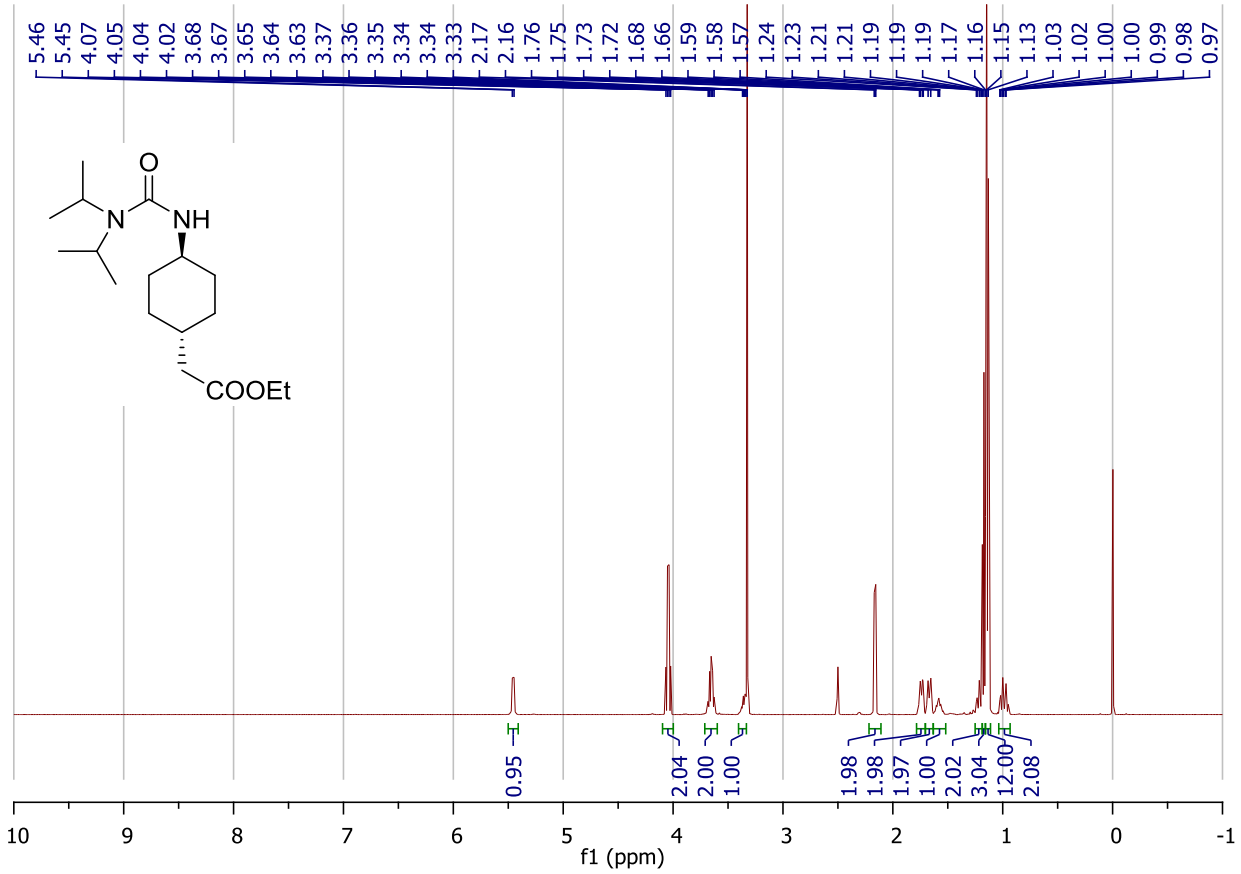


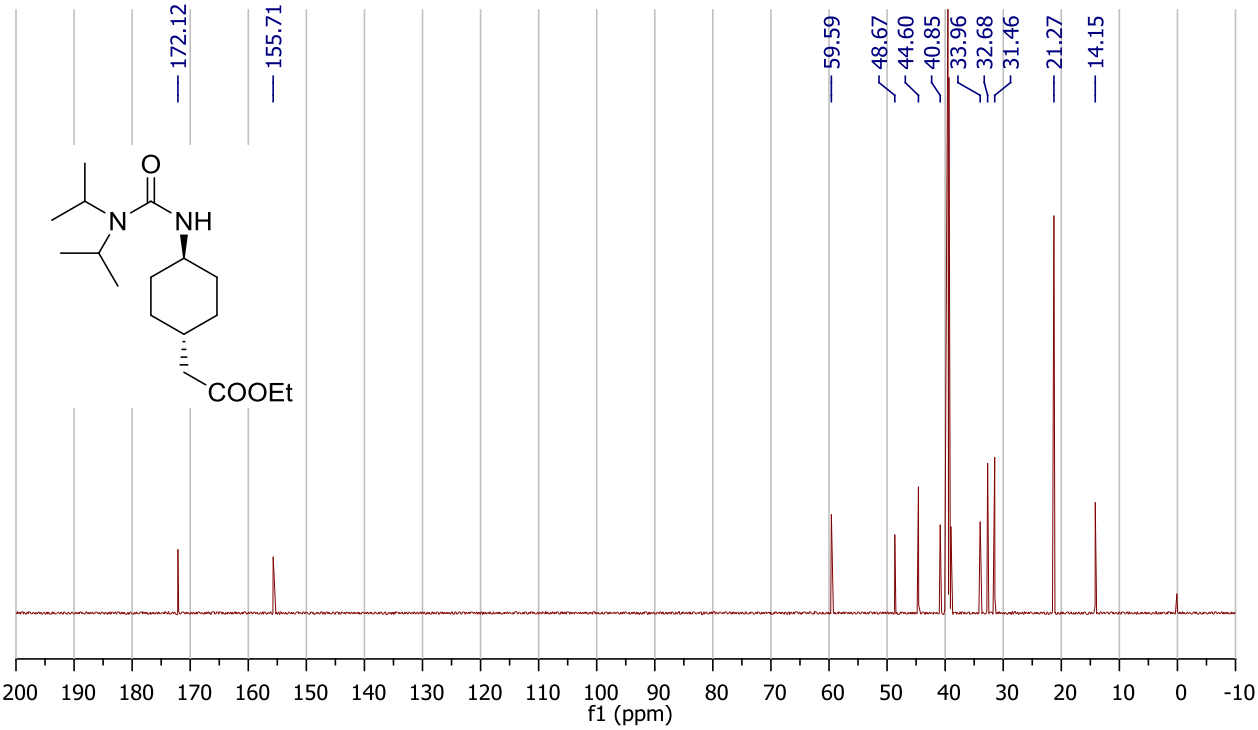

*Cariprazine base (**3**) $^{1}H$ and $^{13}C$ NMR (DMSO + TFA; referenced to DMSO (2.50 ppm in $^{1}H$; 39.50 ppm in $^{13}C$)*

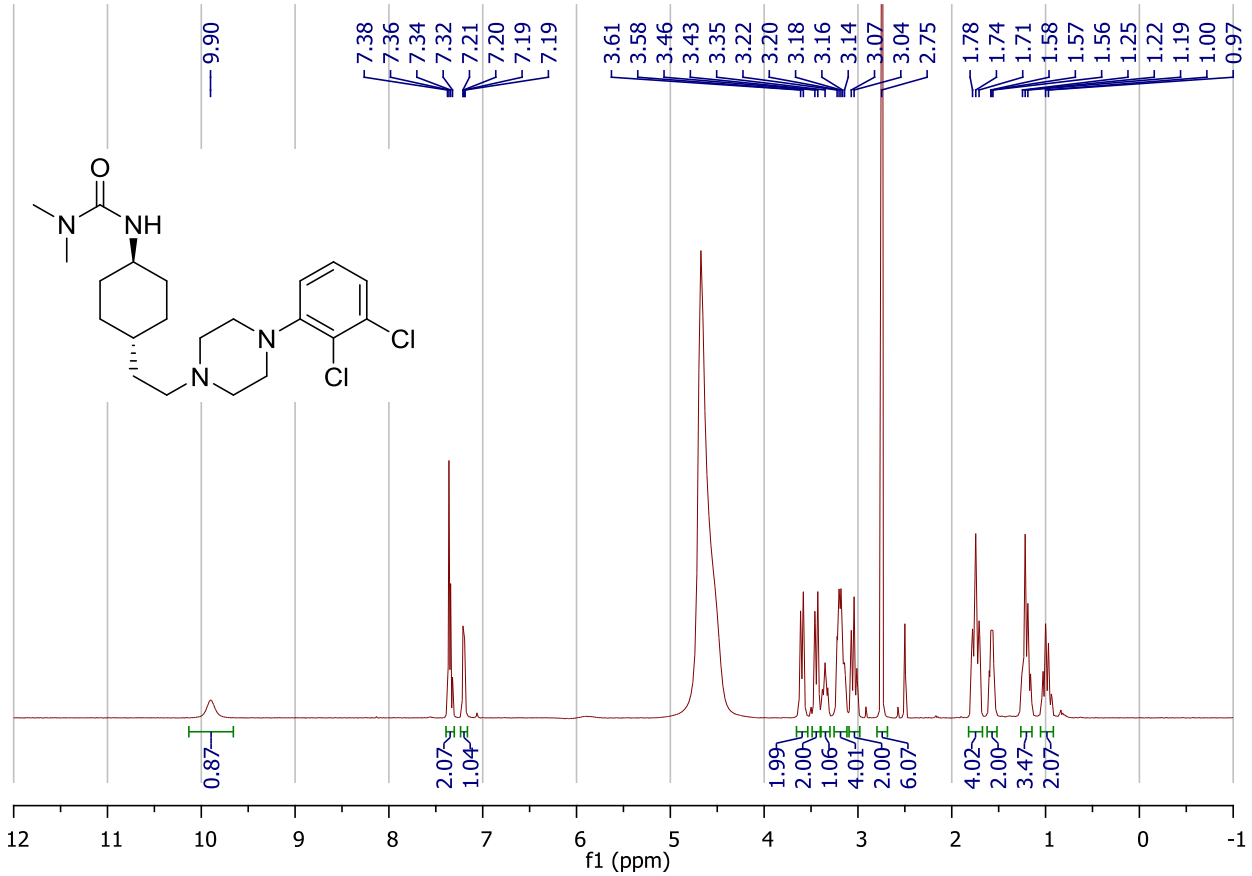


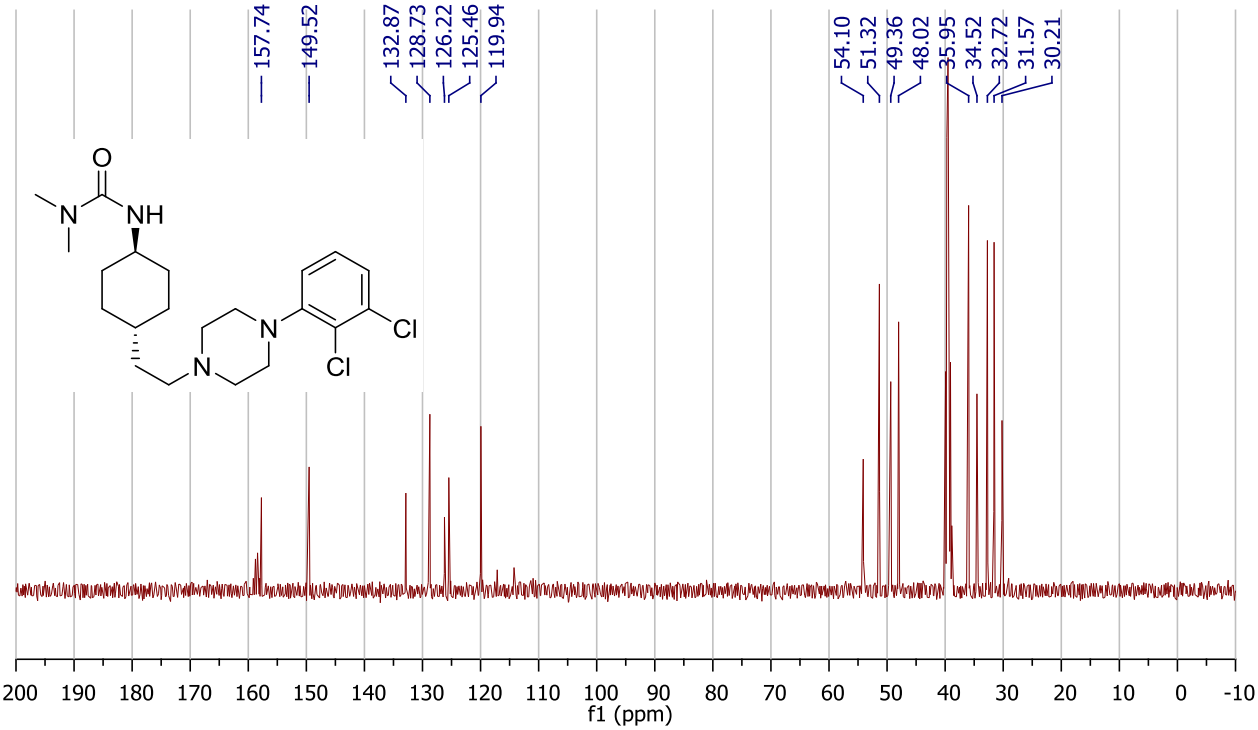

## References


[S1] Y. Matsumura, Y. Satoh, O. Onomura, T. Maki, *J. Org. Chem.* **2000**, *65*, 1549. doi:10.1021/jo991076k

[S2] P. Liu, Z. Wang, X. Hu, *European J. Org. Chem.* **2012**, *2012*, 1994. doi:10.1002/ejoc.201101784

[S3] P.-A. Enquist, P. Nilsson, J. Edin, M. Larhed, *Tetrahedron Lett.* **2005**, *46*, 3335. doi:10.1016/j.tetlet.2005.03.076

[S4] P. Dubé, N. F. F. Nathel, M. Vetelino, M. Couturier, C. L. Aboussafy, S. Pichette, M. L. Jorgensen, M. Hardink, *Org. Lett.* **2009**, *11*, 5622. doi:10.1021/ol9023387

[S5] A. A. Wilson, A. Garcia, S. Houle, O. Sadovski, N. Vasdev, *Chem. Eur. J.* **2011**, *17*, 259. doi:10.1002/chem.201002345

[S6] C. E. Hendrick, Q. Wang, *J. Org. Chem.* **2015**, *80*, 1059. doi:10.1021/jo502541t

[S7] L. Czibula, B. Juhász, É. Ágainé Csongor, F. Sebők, J. Galambos, K. Nógrádi, *WO 2011073705* **2011**.

[S8] J. Shonberg, C. K. Herenbrink, L. López, A. Christopoulos, P. J. Scammells, B. Capuano, J. R. Lane, *J. Med. Chem.* **2013**, *56*, 9199. doi:10.1021/jm401318w

[S9] M. Taddei, E. Cini, M. Rasparini, *WO 2015056164* **2015**.

[S10] X. Chen, F. Ni, Y. Liu, L. Fu, J. Li, *Synthesis* **2016**, *48*, 3120. doi:10.1055/s-0035-1561865